

Analysis of the Transcriptome of Group A *Streptococcus* in Mouse Soft Tissue Infection

Morag R. Graham,* Kimmo Virtaneva,*
Stephen F. Porcella,* Donald J. Gardner,[†]
R. Daniel Long,[†] Diane M. Welty,[†]
William T. Barry,[‡] Claire A. Johnson,*
Larye D. Parkins,* Fred A. Wright,[‡] and
James M. Musser*[§]

From the Laboratory of Human Bacterial Pathogenesis,* Rocky Mountain Veterinary Branch,[†] Rocky Mountain Laboratories, National Institute of Allergy and Infectious Diseases, National Institutes of Health, Hamilton, Montana; the Department of Biostatistics,[‡] University of North Carolina at Chapel Hill, Chapel Hill, North Carolina; and the Center for Molecular and Translational Human Infectious Diseases Research,[§] The Methodist Hospital Research Institute and Department of Pathology, The Methodist Hospital, Houston, Texas

Molecular mechanisms mediating group A *Streptococcus* (GAS)-host interactions remain poorly understood but are crucial for diagnostic, therapeutic, and vaccine development. An optimized high-density microarray was used to analyze the transcriptome of GAS during experimental mouse soft tissue infection. The transcriptome of a wild-type serotype M1 GAS strain and an isogenic transcriptional regulator knockout mutant (*covR*) also were compared. Array datasets were verified by quantitative real-time reverse transcriptase-polymerase chain reaction and *in situ* immunohistochemistry. The results unambiguously demonstrate that coordinated expression of proven and putative GAS virulence factors is directed toward overwhelming innate host defenses leading to severe cellular damage. We also identified adaptive metabolic responses triggered by nutrient signals and hypoxic/acidic conditions in the host, likely facilitating pathogen persistence and proliferation in soft tissues. Key discoveries included that oxidative stress genes, virulence genes, genes related to amino acid and maltodextrin utilization, and several two-component transcriptional regulators were highly expressed *in vivo*. This study is the first global analysis of the GAS transcriptome during invasive infection. Coupled with parallel analysis of the *covR* mutant strain, novel insights have been made into the regulation of GAS virulence *in vivo*, resulting in new avenues

for targeted therapeutic and vaccine research. (Am J Pathol 2006, 169:927-942; DOI: 10.2353/ajpath.2006.060112)

Skin and soft tissue infections are most commonly caused by bacteria and account for ~7 to 10% of hospitalizations in North America.¹ Substantial portions are caused by *Streptococcus pyogenes* (group A streptococci; GAS). A major human pathogen, GAS is associated with millions of skin and throat infections each year.² Serious complications after infection, namely rheumatic fever, glomerulonephritis, and reactive arthritis, can follow even relatively mild GAS infections and cause significant morbidity worldwide.^{3,4} Some GAS infections rapidly progress to life-threatening invasive diseases such as septicemia, streptococcal toxic shock syndrome, and necrotizing fasciitis, requiring life-saving interventions in the form of aggressive fluid replacement, general supportive measures, and/or emergent surgical debridement.²⁻⁴ Nearly 15,000 cases of invasive GAS disease and an estimated 1300 deaths occur annually in the United States.⁵ Epidemiological data also suggest increased incidence and severity of GAS infections in recent years.^{2,6,7} Because progression to systemic toxicity and shock can occur throughout a span of hours, early recognition and initiation of aggressive therapies are essential.

Molecular mechanisms mediating GAS-host interactions remain poorly understood but are crucial for rapid diagnostic, therapeutic, and vaccine development.^{3,4} As a consequence, concerted efforts have been made to identify regulatory mechanisms involved in coordinating the *in vitro* expression of GAS virulence determinants. Genes have been identified that regulate production of proven and putative virulence factors, and several of these regulators are known to respond to environmental changes *in vitro* or to

Supported in part by National Institute of Allergy and Infectious Diseases intramural funding.

Accepted for publication May 10, 2006.

Supplementary material for this article can be found on <http://ajp.amjpathol.org>.

Address reprint requests to James M. Musser, M.D., Ph.D., Center for Molecular and Translational Human Infectious Diseases Research, The Methodist Hospital Research Institute, and Department of Pathology, Methodist Hospital, 6565 Fannin St., B490, Houston, TX 77030. E-mail: jmmusser@tmh.tmc.edu.

specific phases of the bacterial growth cycle.^{3,8} However, far less is known about gene expression *in vivo* during GAS infection of mammalian hosts.^{9–11} Infection sites or the host circulation environment are complex, and their influence on bacterial gene regulation cannot be simulated *in vitro*.¹² Hence, further understanding of GAS host/pathogen molecular interactions requires analysis of *in vivo* conditions that better approximate the natural history of infections.

Streptococcal soft tissue infections, such as cellulitis involving the subdermal layers and superficial fascia, often commence with nonspecific symptoms such as erythema, heat, soft tissue edema, generalized pain, and sometimes serosanguinous bullae.^{6,7} Progression to diffuse necrosis of subcutaneous and deep fascia (necrotizing fasciitis) often occurs without overt skin injury¹³ and leads to development of vasculitis, intravascular thrombosis, and tissue gangrene. Histopathology of debrided soft tissue reveals acute inflammation of subcutaneous tissue with bacterial aggregates and multifocal necrosis. Mice subcutaneously injected with GAS also develop inflamed bullae that later ulcerate; diffuse inflammatory infiltrates with high bacterial counts, and diffuse tissue necrosis including thrombosed vessels.³ In a previous study,¹⁴ we measured a subset ($n = 17$) of GAS transcripts expressed *in vivo* 2 days after inoculation with a wild-type (WT) serotype M1 GAS strain and a $\Delta covR$ isogenic deletion mutant of a key GAS two-component regulatory system (TCS) referred to as CovR-CovS (Cov, control of virulence). In this present study we have expanded our investigation by using a custom high-density array for whole GAS transcriptome analysis in the murine soft tissue infection model. The data presented here provide substantial new information about GAS survival strategies in soft tissue. The most abundant GAS transcripts detected were found to encode extracellular proteins that are key virulence determinants. Other expressed GAS genes are potential targets for therapeutic intervention and warrant further study.

Materials and Methods

Bacterial Strains

Serotype M1 GAS strains commonly cause pharyngitis and invasive infections.² Strain MGAS5005 (no. BAA-947; American Type Culture Collection, Rockville, MD), a WT clinical strain (serotype M1), and its isogenic $\Delta covR$ derivative strain (JRS950) have been described.^{14–16} Bacteria were cultured statically on Trypticase soy agar containing 5% sheep blood agar (Becton-Dickinson, Cockeysville, MD) or in Todd-Hewitt broth (Becton-Dickinson) containing 0.2% (w/v) yeast extract (THY; Difco Laboratories, Detroit, MI), at 37°C in an atmosphere containing 5% CO₂. For generating inoculum, cells were harvested from THY at late-exponential phase (OD₆₀₀ ~0.75) to limit infectivity differences across strains associated with up-regulated capsule biosynthesis in strain JRS950, which is maximal in the early-to-mid exponential growth phases.

Mouse Soft Tissue Infection Model

This model of GAS soft tissue infection has been used extensively to study bacterial-host interactions.^{14,17,18} Our experimental protocol was approved by the Institutional Animal Care and Use Committee, National Institute of Allergy and Infectious Diseases. Outbred, immunocompetent, hairless male Crl:SKH1-hrBR mice (5 weeks old; 20 to 25 g) (Charles River Breeding Laboratories, Bar Harbor, ME), maintained on standard mouse food and water *ad libitum*, were randomly assigned to one of two treatment groups (WT or $\Delta covR$ mutant GAS strain, $n = 27$ each; four mice per cage). Immediately before inoculation, the animals were weighed and anesthetized with isoflurane (Aerrane; Ohmeda Caribe, Guayama, Puerto Rico) inhalation. The animals were inoculated subcutaneously in the dorsal side with 0.1 ml of pyrogen-free phosphate-buffered saline (PBS) (diluent) or $\sim 3 \times 10^7$ colony-forming units of MGAS5005 (WT) or JRS950 ($\Delta covR$). The actual colony-forming units of viable bacteria inoculated were verified by growth on blood agar.

To blind the investigator, cage numbers were reassigned after inoculation, and the blind was broken after data analysis. Methods for clinical measurements and analysis of gross pathologies have been reported previously for this soft tissue model of infection,^{14,19} and data are found in Supplementary Tables 1 and 2 (see <http://ajp.amjpathol.org>). Length (L) and width (W) values were used to calculate abscess volume [$V = 4/3\pi(L/2)^2 \times (W/2)$] and area [$A = \pi(L/2) \times (W/2)$], using equations for a spherical ellipsoid as described.¹⁴

At 53 hours after inoculation, mice were euthanized and weighed, the infection site was swabbed to confirm GAS infection, and tissue was obtained from each animal via a biopsy that included dermis and underlying soft tissue lesions. Tissues were wrapped in aluminum foil, snap-frozen in liquid nitrogen, and stored at -80°C until RNA was isolated. Three additional control mice injected with sterile saline failed to show symptoms of clinical infection and did not grow GAS bacterial colonies on plating.

Experimental Design

A one-factor experimental design with two treatment (strain) levels was used. Samples were randomized at the start of procedures, and care was taken to ensure that batches of sample preparation, array hybridizations, and posthybridization washes were not confounded with treatment. Additional experimental design details are outlined in the Supplementary Materials and Methods (see <http://ajp.amjpathol.org>).

RNA Isolation

Frozen tissue extracts were divided into three aliquots from which RNA was purified. Tissue extracts were pulverized with a series of sharp blows delivered with a 3-pound drill hammer (Razor-Back; Union Tools Inc., Columbus, OH). Cell lysis and RNA isolation were conducted with a FastRNA kit (MP Biomedicals, Irvine, CA)

as described.²⁰ The concentrate was fragmented with a Qiashredder (Qiagen, Inc., Valencia, CA) and the isolated total RNA (containing both bacterial and host RNA) was purified in 96-well format using a plate centrifugation system (RNeasy 96; Qiagen), with on-column DNase I treatment and posttreatment with DNAFree (Ambion, Inc., Austin, TX) as described.^{10,20} RNA integrity was assessed with a 2100 bioanalyzer (Agilent Technologies, Palo Alto, CA)^{10,20} and by measurement of the A_{260}/A_{280} ratios. Absence of contaminating bacterial genomic DNA was confirmed by real-time polymerase chain reaction (PCR). Two RNA aliquots were pooled to perform the microarrays; the remaining extract was used for real-time RT-PCR validation.

Bacterial Target Preparation

Fifty-four microarray targets were prepared primarily as described.^{10,20} Briefly, each RNA sample was divided into two to three aliquots of 10- μ g total RNA (each) to which 0.8 μ g of bacteriophage MS2 carrier RNA (Roche Applied Biosciences, Indianapolis, IN) was added. Control spike transcripts (130 pmol/L) were added to each RNA aliquot, and 5 μ g of random primers (Invitrogen, Carlsbad, CA) were annealed (10 minutes at 70°C, 10 minutes at 25°C). cDNA synthesis reactions and postsynthesis RNA digestion were performed as described.^{10,20} In brief, the resultant cDNA was purified using Qiaquick 96 kit (Qiagen) according to the manufacturer's recommendation. For cDNA fragmentation, 3 μ g of cDNA and 0.75 U of DNase I (Roche Biosciences) were used (10 minutes at 37°C, 10 minutes at 98°C). The desired cDNA size range of 50 to 200 bases was verified by separating 200 ng of cDNA on a RNA 6000 Nano LabChip (Agilent) using the 2100 BioAnalyzer (Agilent) with no added dye in the loading buffer. The fragmented cDNA was then end-labeled with biotin-ddUTP as per the Enzo BioArray terminal labeling kit (60 minutes at 37°C; Enzo Diagnostics, New York, NY) and pooled with other end-labeled cDNAs of the same sample. Samples were hybridized to 54 Rocky Mountain Laboratory (RML) Affymetrix custom GAS arrays, as described.^{10,20}

Affymetrix GeneChip Custom Array

The Affymetrix Inc. (Santa Clara, CA) custom high-density anti-sense oligonucleotide GeneChip array (designated RMLChip herein) has been described.^{10,16} It contains redundant probe sets representing more than 90% coverage of predicted coding regions (1869 ORFs) encoded by the MGAS5005 genome.¹⁶ Each probe set is used to detect the presence of a single transcript, and several GAS transcripts (genes) are represented by more than one probe set. For in-depth RMLChip details, refer to the Supplementary Materials and Methods (see <http://ajp.amjpathol.org>).

GeneChip Hybridization

Target hybridizations, washing, staining, and scanning were performed by the National Institute of Allergy and

Infectious Diseases Affymetrix core facility (Science Applications International Corp., Frederick, MD) using a GeneChip hybridization oven and the *Pseudomonas aeruginosa* hybridization protocol (Affymetrix), as described.²⁰ The hybridization solution volume used was 200 μ l because the RMLChip is a standard size array. Each array was scanned at 570 nm at 3- μ m resolution with a GeneArray scanner. Scanned DAT-image files were analyzed with Affymetrix Microarray Suite (MAS) 5.0 software. The raw CEL files have been submitted to Gene Expression Omnibus (<http://www.ncbi.nlm.nih.gov/geo>). Downstream genome analysis was accomplished using MicrobesOnline (available at <http://www.microbesonline.org>)²¹ and in-house bioinformatics analysis.

Statistical Analysis

Model-based expression estimates for each gene were obtained using the PM-MM difference model²² of dCHIP software as described.²⁰ The gene expression estimates were normalized across samples by quadratic scaling to an artificial array with the median expression for each gene.²³ Two-dimensional scatterplots of expression estimates were generated for all pairs of samples within the same treatment group to examine uniformity across samples. Hierarchical clustering and principal components analyses also were performed (Supplementary Figure 1, see <http://ajp.amjpathol.org>). Five arrays with poorer quality RNA and low within-strain correlation were removed as outliers. Downstream data analysis was performed with MGAS5005 genome-specific probe sets using Partek Pro (Partek Inc., St. Louis, MO). To evaluate expression rankings, absolute square root-transformed expression estimates were integer-ranked, starting from 1 for the most abundant GAS transcript and increasing correspondingly with decreasing transcript detection. To investigate expression correlations, standard Pearson correlation coefficients were determined for select genes versus all other genes using Partek Pro. To investigate strain effects, expression estimates were analyzed by analysis of variance with treatment (WT versus Δ *covR* strain) as a fixed effect. Technical variables included in the analysis included batches for sample preparation, sample hybridization, and posthybridization washes (Supplementary Figure 2, see <http://ajp.amjpathol.org>). Final results were subjected to multiple testing correction using $Q \leq 0.05$ false discovery rate cutoff values.^{24,25} Using rigorous permutation-based statistics, we also performed significance analysis of function and expression (termed SAFE)²⁶ to assess the significance of multiple gene categories in GAS *in vivo* transcriptional responses across strains. A detailed description of the procedures used is provided in the Supplementary Materials and Methods (see <http://ajp.amjpathol.org>).

Quantitative Real-Time Reverse Transcriptase (RT)-PCR Analysis

Real-time reverse transcriptase (RT)-PCR assays were conducted to validate a subset of the microarray data.

Eight oligonucleotide primer pairs and 6FAM-labeled probe sets (specific for *cfa*, *dppA*, *emm1*, *scaD*, *sclA*, *sic*, *slo*, and *speA2*) were used to perform target amplification and detection from cDNA templates in 20- μ l multiplex two-step RT-PCR reactions as described.²⁰ Targets were selected to encompass the full range of expression signal values identified by array transcriptome analysis. Target abundance was normalized to JOE-labeled internal reference transcript *proS*, which is transcribed at constant levels throughout the GAS growth cycle *in vitro* and not affected by *covR* inactivation.¹⁴ Differences in median values were evaluated for statistical significance with the Mann-Whitney rank sum test at the $P \leq 0.001$ level.

Sampling and Histological Assessment

Tissue used for histological examination was prepared from mice subcutaneously inoculated with 2.4×10^7 colony-forming units of GAS strains MGAS5005 or Δ *covR* JRS950 ($n = 16$, each strain) as described above, except that 4-week-old (15 to 20 g) female Crl:SKH1-*hrBR* mice (Charles River Breeding Laboratories) were used. Six animals inoculated with PBS were used as controls. For assessment of bacterial content, histopathology, and bacterial protein expression, mice were euthanized 48 hours after inoculation, and the skin and underlying soft tissue were removed from inoculation sites and fixed in 10% buffered formalin before embedding in paraffin. To assess the presence of bacteria and pathological changes, formalin-fixed tissues were sectioned and stained with gram stain or hematoxylin and eosin (H&E) stain (Sigma, St. Louis, MO), according to standard methodologies. An Olympus model BX51 microscope equipped with a Q-FIRE (Olympus, Tokyo, Japan) camera was used for image capture.

Immunohistochemical Analysis

Rabbit polyclonal anti-GAS antibodies made against purified recombinant GAS proteins²⁷ were used for immunostaining. Paraffin-embedded tissues were cut into 4- μ m sections and stained with antibodies specific for 16 bacterial antigens [M5005_Spy ORF numbers designated in square brackets] (AtmB [0271]; PrtS [0342]; MtsA [0368]; IdeS/Mac [0668]; [0942]; PstS [0955]; SpeA2 [0996]; MalE [1058]; PrsA [1133]; [1308]; HtsA/SiaA [1528]; Shp [1529]; DppA [1704]; Lmb [1711]; Fba [1713]; SIC [1718]) using biotinylated secondary antibodies in combination with horseradish peroxidase-coupled streptavidin (DAKO Corp., Carpinteria, CA) and the substrate AEC (BioGenex, San Ramon, CA). To evaluate nonspecific staining, a polyclonal antibody recognizing a control peptide (Bethyl Laboratories, Montgomery, TX) was used as negative control. The M3.1/1-24 control peptide, representing the N-terminal peptide of serotype M3 Emm3.1, was used because this peptide is not encoded within the genome of the serotype M1 WT strain MGAS5005.¹⁶ All immunohistochemically (IHC) stained sections were counterstained with Mayer's hematoxylin and mounted using synthetic aqueous-based mounting medium (DAKO Faramount).

Results

Gross and Microscopic Pathology

PBS-inoculated skin sections from the immunocompetent Crl:SKH1-*hrBR* mice were histologically normal whereas animals inoculated with either WT or Δ *covR* strain demonstrated subcutaneous foci of suppurative inflammation with adjacent infiltrating polymorphonuclear lymphocytes (PMNs), dermatitis, loss of stratum corneum, fibrin thrombi in the small vessels, and varying degrees of dermal and epidermal necrosis with degenerate and necrotic neutrophils (Figure 1). Δ *covR*-inoculated mice had more extensive inflammation (panniculitis), ulcerated epidermis and necrosis of subcutaneous tissue fascia with some areas of muscle involvement (myonecrosis), and faster ulcer development (Figure 1), thus confirming previous reports of the hypervirulence of Δ *covR* mutant GAS strains. All gram stains of infected tissues revealed aggregates of gram-positive cocci in multiple focal planes (Figure 2). Taken together, these observations provide histopathological evidence of high bacterial loads and diffuse tissue necrosis analogous to progressive human infections.

Abundant in Vivo GAS Transcripts

The vast majority of the top 200 detected GAS transcripts in WT-inoculated tissue extracts from soft tissue infection encode products involved in protein synthesis ($n = 22$), information processing ($n = 15$), carbohydrate metabolism ($n = 15$), membrane transport ($n = 15$), stress adaptation ($n = 15$), or cellular processing ($n = 14$) are shown in Supplementary Table 3 (see <http://ajp.amjpathol.org>) and discussed in more detail below. In addition, transcripts with virulence ($n = 10$), cell wall metabolism ($n = 8$), and unknown functional annotation ($n = 9$) also were detected at high levels (Supplementary Table 3, see <http://ajp.amjpathol.org>) implying that replication, protein synthesis, cellular remodeling, and stress adaptation are important functions during soft tissue infection. Proteins encoded by five GAS transcripts found to be abundant in the infected tissue [penicillin-binding protein (PBP) 1A (*pbp1a*), a protein translation initiation factor (*tdcF*), a putative lipoprotein (*atmB*), a hypothetical protein of unknown function (M5005_Spy1104), and DNA polymerase III (*polC*) involved in DNA replication] have been previously detected by *in vivo*-induced antigen technology (IVIAT) using convalescent human and mouse²⁸ sera.

The virulence-associated *sic* and *emm* transcripts, encoding the anti-phagocytic extracellular streptococcal inhibitor of complement (SIC) and hypervariable surface antigen designated M protein, ranked within the top seven most abundant transcripts in WT-inoculated animals and within the top 11 in mutant-inoculated mice (Supplementary Table 3, see <http://ajp.amjpathol.org>). Six cotranscribed ORFs (M5005_Spy0971-6), encoding hypothetical and general stress proteins related to Gls24 of *Enterococcus faecalis*, were among the 20 most highly expressed GAS transcripts detected with both inoculating strains, an important finding given that Gls24 may be

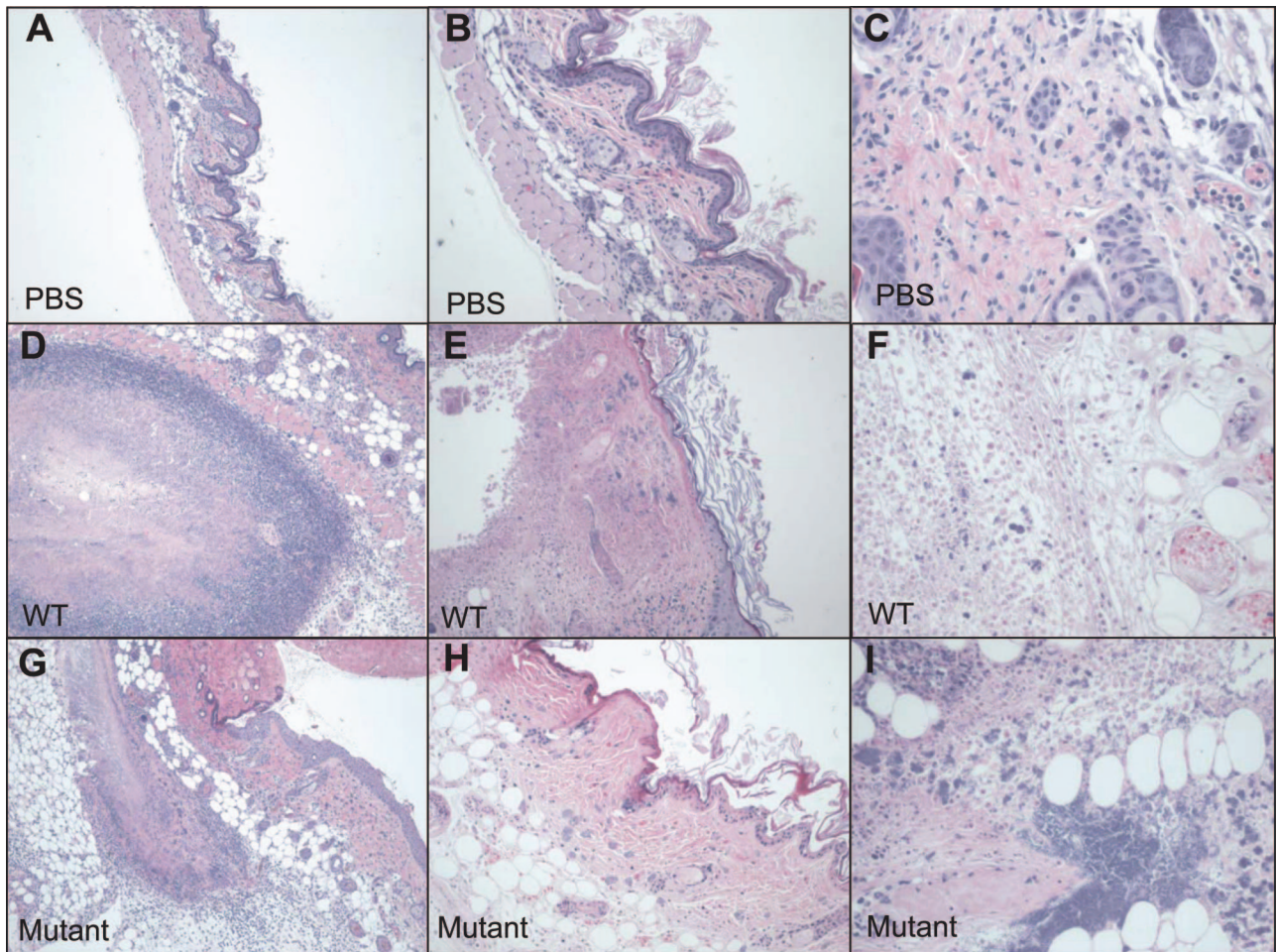


Figure 1. Histopathological assessment of GAS mouse skin infection. Photomicrographs of H&E-stained, formalin-fixed tissue biopsies taken from PBS-inoculated (control) animals (top row), strain MGAS5005 (WT)-infected animals (middle row), and animals infected with $\Delta covR$ mutant strain JRS950 (bottom row) at 2 days after inoculation. Results are representative of tissues obtained from animals in each of the groups. Additional histopathology and gram stains of biopsies from the same animals (**D**, **G**) are depicted in Figure 2, B and E and C and F, respectively. Original magnifications: $\times 40$ (**A**, **D**, **G**); $\times 100$ (**B**, **E**, **H**); $\times 200$ (**C**, **F**, **I**).

important for virulence in the murine invasive model of *S. pneumoniae* infection.²⁹ Other high-level GAS transcripts detected in WT-infected tissues include the chromosomal *spd* locus (ranked 14th) encoding a secreted DNase¹⁷; *sagA* (ranked 28th) encoding a potent host cytolysin called streptolysin S (SLS); *dppA* (ranked 47th) encoding dipeptide binding protein; *gap/plr* (ranked 71st) and *eno* (ranked 117th) encoding glycolytic enzymes glyceraldehyde 3-phosphate dehydrogenase (GAPDH) and α -enolase, respectively; *scpA* (ranked 84th) encoding C5a peptidase; *spyCEP* (ranked 97th) encoding an IL-8-cleaving surface proteinase³⁰; *lmb* (ranked 192nd) encoding a laminin-binding surface adhesin,³¹ and *spyA* (ranked 211th) encoding an ADP-ribosyl transferring exotoxin that disrupts host cell cytoskeletal structures.³² Several GAS regulatory genes also had highly expressed transcripts, including the repressor of class I heat shock genes *hrcA*³³ (ranked 15th), transcriptional regulator RofA (ranked 30th) involved in modulating adhesin expression,⁸ ferric iron transport regulator PerR³⁴ (ranked 130th), and the TCS designated *lkh/lrr* (ranked 162nd/288th), which is essential to GAS survival responses during PMN interactions.³⁵ Among the top 200 detected

GAS transcripts, 20 encode for products predicted (by their amino acid sequences) as cell surface-associated or secreted, whereas transcripts encoding experimentally confirmed extracellular gene products such as SIC, streptodornase (ranked 14th), Mn²⁺-binding surface lipoprotein designated MtsA (ranked 88th), and an immunogenic secreted protein designated Isp2 (ranked 188th) also were observed.

GAS Protective Response Augmented in the Soft Tissue Environment

As described above, we detected elevated transcript levels in WT-infected mouse tissues for genes involved in oxidative stress protection and stress adaptation. These transcripts also included genes encoding the reactive oxygen-reducing enzymes superoxide dismutase SodA (ranked 114th),³⁶ peroxiredoxin reductase AhpC and AhpF (ranked 115th and 147th),³⁷ and NADH oxidase NOX (ranked 129th),³⁸ molecular scavengers such as the antioxidant Dpr protein (ranked 76th),³⁹ *clpC* (ranked 158th) encoding heat shock protease ClpC involved in

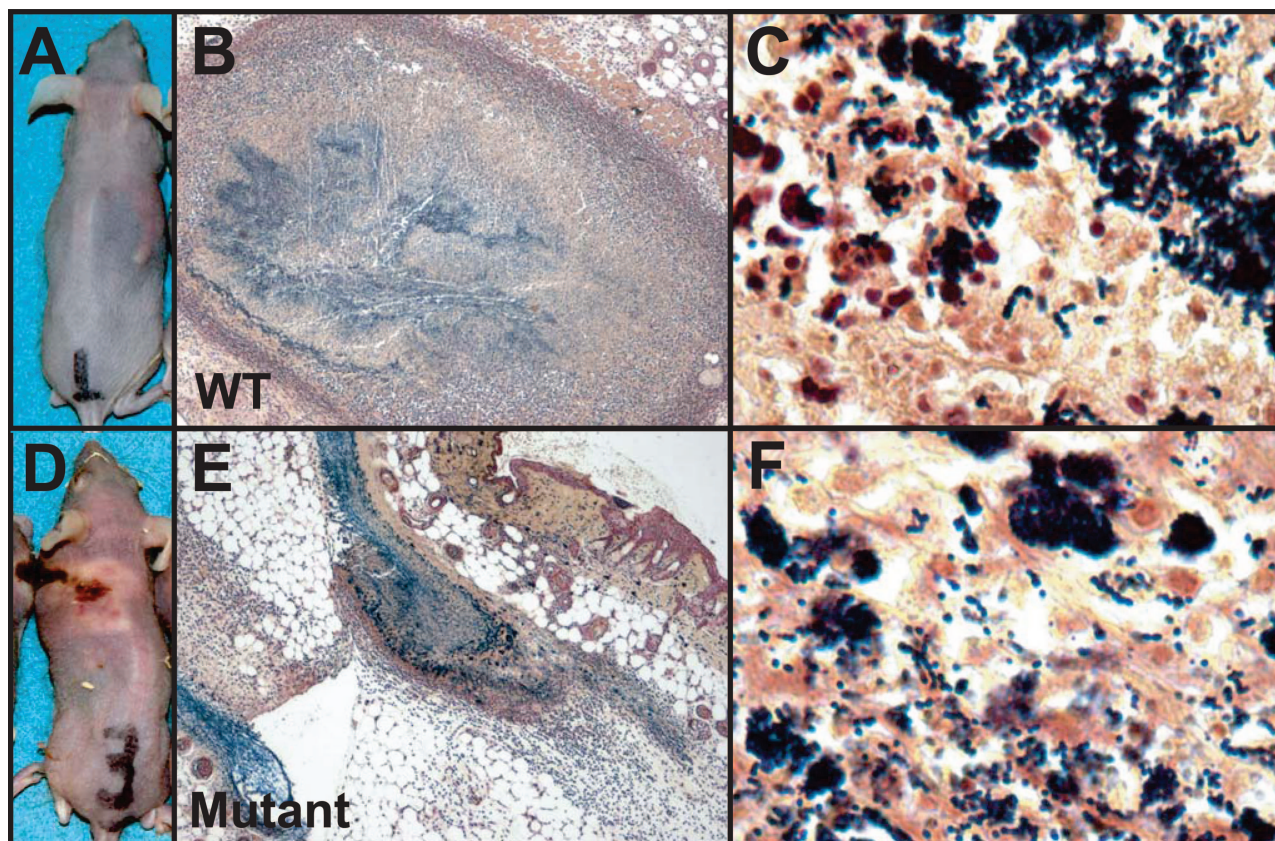


Figure 2. Gram stains of GAS during invasive soft tissue infection. Depicted are gram-stained skin tissue sections from mice infected with WT GAS strain MGAS5005 (**B, C**) and $\Delta covR$ mutant strain JRS950 (**E, F**). Also shown are the external pathologies for the same animals infected with WT (**A**) and $\Delta covR$ mutant (**D**). IHC analyses of biopsies from the same animals are depicted in Figure 5, B (WT) and D (Mutant), respectively. Original magnifications: $\times 40$ (**B, E**); $\times 100$ (**C, F**).

tolerance to environmental stress,⁴⁰ *recA* (ranked 169th) encoding the RecA regulator of bacterial SOS responses, and sortase SrtA (ranked 131st) involved in the maturation of extracellular GAS proteins. Molecular chaperones as well as DNA and protein repair functions (chaperone proteases) also were elevated in soft tissues (Supplementary Table 3, see <http://ajp.amjpathol.org>). Importantly, we also detected abundant transcripts encoding products involved in GAS cell wall formation and modification, including the murein transpeptidase-transglycosylases PBP 1B and PBP 2A (ranked 29th and 149th, respectively) and UDP-*N*-acetylmuramate-alanine ligase (*murC*; ranked 151st) among others suggesting an important role in cell wall modifications or repair during tissue infection.

Co-Expressed Transcripts

Numerous *in vitro* studies have demonstrated that *emm*, *sic*, and *mga* are coregulated by the multigene transcriptional activator called Mga. High correlation ($r > 0.9$) between co-expressed transcripts suggested that in addition to *emm*, *sic*, and *mga*, chromosomally adjacent genes M5005_Spy1721-8 also are likely Mga regulon members (Supplementary Table 4, see <http://ajp.amjpathol.org>). These adjacent coding regions contain an immunogenic secreted protein designated Isp; the Ihk/Irr

TCS; and members of an ATP-binding cassette transport system of unknown function. High correlation ($r = 0.91$) between transcripts also was observed between *eno*, encoding the surface-localized glycolytic enzyme α -enolase, and *emm* encoding the anti-phagocytic M1 protein (data not shown). The latter represents an interesting and new observation because these genes are distant on the GAS chromosome, yet both encode proteins that interact directly with host plasminogen.⁴¹

Analysis of Strain Effect in the Soft Tissue Environment

GAS transcript correlations with transcription of *covR/S* are shown in Supplementary Table 5 (see <http://ajp.amjpathol.org>). In total, 76 GAS transcripts were differentially expressed across WT versus *covR* mutant in the lesions ($Q < 0.05$; $P < 0.002$; Figure 3; Supplementary Table 3; Supplementary Figures 3 and 4, see <http://ajp.amjpathol.org>). CovR acts as a transcriptional repressor^{14,20,42-44}, and therefore it was not unexpected that the vast majority ($n = 50$) of differentially expressed transcripts were more abundant in tissues infected by the $\Delta covR$ strain as compared with the WT-type strain. Genes or transcripts up-regulated as compared with WT conditions (1.4-fold to 2.8×10^3 -fold higher expression) en-

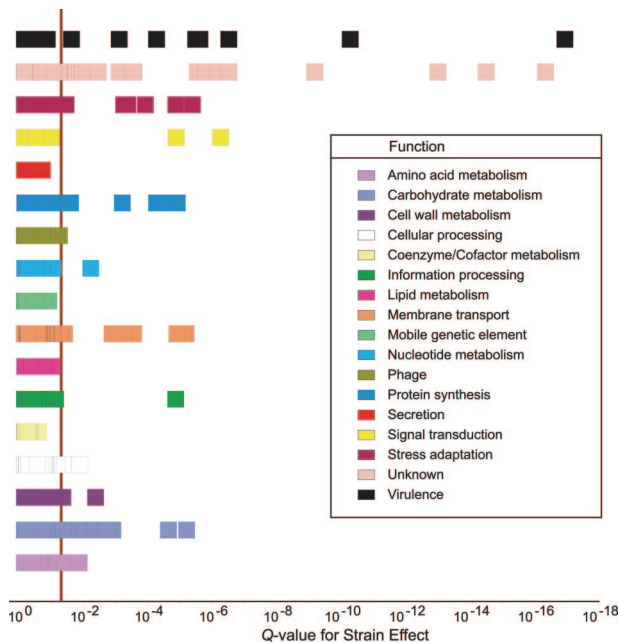


Figure 3. Analysis of variance revealed a significant strain effect in the *in vivo* microarray expression data. The depicted box plot shows the confidence of calls for strain effect in *Q* values (*P* values adjusted for multiple testing using false discovery rate) on the horizontal axis versus GAS functional category. A vertical line delineates the statistical significance threshold ($Q < 0.05$) for differentially expressed GAS transcripts in WT versus $\Delta covR$ mutant strain. The 76 identified differential transcripts in the *in vivo* transcriptome data are primarily associated with carbohydrate metabolism, membrane transport, signal transduction, stress adaptation, unknown functions, and virulence.

coded the secreted DNase streptodornase (*spd*); plasminogen activator streptokinase (*ska*); cysteine protease (*speB*), and the entire streptolysin S (SLS) biosynthesis locus (*sagA-l*). Up-regulated transcripts in the $\Delta covR$ mutant are generally associated with unknown functional annotations ($n = 14$), but only six were common with up-regulated transcripts after *ex vivo* blood culture.²⁰ However, carbohydrate metabolism ($n = 9$); virulence ($n = 8$), and membrane transport ($n = 7$) functions also were statistically more significantly up-regulated than in the WT. Noteworthy up-regulated transcripts include genes coding for the 67-kd myosin-crossreactive streptococcal antigen (M5005_Spy0385); hyaluronan (capsule) synthesis enzyme HasA, and a cell wall-modifying enzyme peptidoglycan amidohydrolase (M5005_Spy0500). Conversely, one third of differentially expressed transcripts ($n = 26$) were significantly less abundant in $\Delta covR$ versus the WT-inoculated tissues (1.5- to 12.6-fold reduced expression; Supplementary Table 3, see <http://ajp.amjpathol.org>). To further investigate transcriptome differences between WT and *covR*-minus, we analyzed functional categories that were overrepresented by gene-specific analysis based on 10,000 permutations of array assignments, a process previously described.²⁶ Sixty-five GAS transcripts achieved the minimum cutoff value (false discovery rate ≤ 0.003). Numerous GAS transcripts encoding virulence-associated extracellular products exhibited overexpression in $\Delta covR$ -inoculated tissues versus WT (Supplementary Figure 5; Supplementary

Table 6, see <http://ajp.amjpathol.org>), a finding seen previously in *in vitro* experimental conditions.^{14,20} In contrast, most transcripts involved in stress adaptation were underexpressed in $\Delta covR$ - versus WT-inoculated tissues (Supplementary Figure 6; Supplementary Table 6, see <http://ajp.amjpathol.org>), suggesting that although CovR acts primarily as a transcriptional repressor for tissue damaging virulence factors, lack of this repression may mean less stress adaptation is required within the localized environment. Virtually no transcripts were detected for the activator of CovR expression (designated RocA; Supplementary Table 3, see <http://ajp.amjpathol.org>) suggesting that CovR is modulated *in vivo*. Although we detected mid-range levels of transcripts encoding CovR (ranked 269th) in WT-infected tissues, CovR phosphorylation status determines its DNA-binding (repressing) activity.⁴⁵

Validation of Oligonucleotide-Array Gene Expression (Transcript) Results

To validate the microarray data, we performed quantitative reverse transcription RT-PCR (TaqMan) assays with eight selected GAS transcripts (Figure 4). The transcript detection rank orders were nearly identical with only *dppA* and *speA* reciprocated across the two methods (in rank order of abundance: *sic*, *emm*, *dppA*, *slo*, *sceD*, *sclA*, *speA*, *cfa* in microarray dataset (Figure 4A) versus *emm*, *sic*, *speA*, *slo*, *sceD*, *sclA*, *dppA*, *cfa* by TaqMan analysis (Figure 4B). TaqMan assays detected much higher levels of *speA* transcripts encoding the pyrogenic toxin superantigen PTSAg SpeA2, possibly resulting from use of the single endogenous transcript (*proS*) in TaqMan assays as opposed to use of all transcripts for normalizing microarrays. Strong positive correlation ($r = 0.87$) was observed overall for expression measurements obtained by the two methods, and for all transcripts, concordance was observed between methods for the direction (increase versus decrease) of expression differences across inoculating GAS strains.

Immunohistochemical Analysis of Mouse Tissue

In situ IHC with specific antibodies directed against 16 GAS proteins was used to detect proteins made from identified transcripts. Absence of specific staining in negative control tissues confirmed lack of antibody cross-reactivity (Figure 5). Seven of the 16 GAS-specific antibodies were reactive *in situ* with several GAS antigens demonstrating high levels of immunoreactivity or abundance (Figure 5; Supplementary Table 7, see <http://ajp.amjpathol.org>). Our detection of immunoreactivity of PrsA protein (M5005_SPy1133; ranked 121st transcript) supports previous observations of *in vivo* expression of a PrtM homolog involved in protease maturation,²⁷ a significant note, given that PrtM-immunized mice are protected against *S. pneumoniae* infection.⁴⁶ Despite limited detection of *malE* RNA transcripts (M5005_Spy1058; ranked 561st); a surprisingly high degree of immunoreactivity was observed for the solute-binding surface lipoprotein

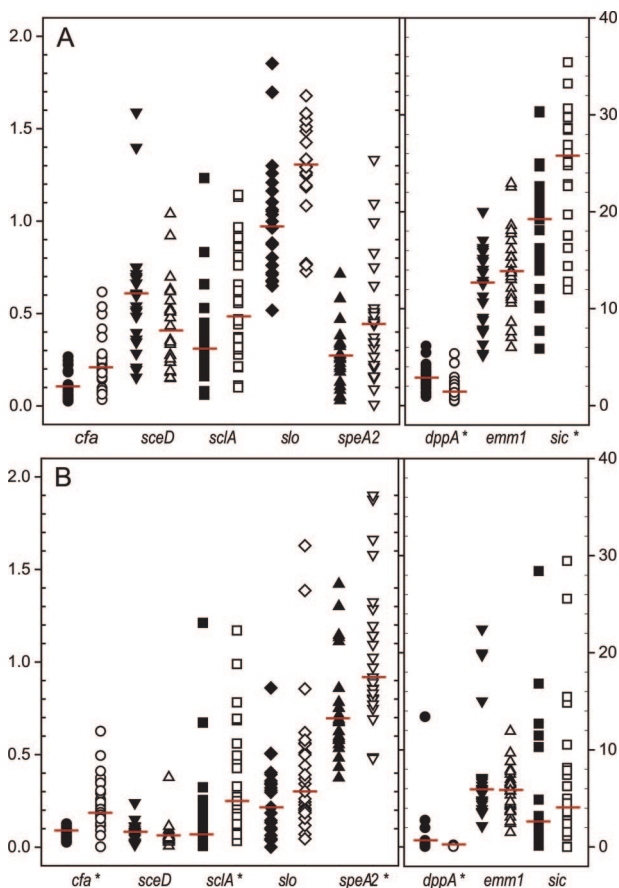


Figure 4. Verification of representative oligonucleotide microarray transcriptome data. Depicted are GAS expression estimates for eight selected GAS transcripts, as obtained by RMLChip microarray experiments (A) and real-time RT-PCR (TaqMan) assays (B). Results depicted summarize the analysis of 49 mice infected with either WT strain MGAS5005 ($n = 23$; closed symbols) or the isogenic *covR* mutant ($n = 26$; open symbols) and are expressed as median expression relative to the reference transcript *proS* (M5005_spy1673). Asterisks depict transcripts detected as differentially expressed at $Q \leq 0.001$ in arrays (A) and in TaqMan assays at $P \leq 0.001$ according to the Mann-Whitney rank sum test (B).

MalE, known to be involved in maltodextrin/maltosaccharide uptake (see below). Immunoreactivity also was noted in the IHCs for the extracellular virulence-associated proteins PTSAg SpeA2 (M5005_Spy0996) and SIC (Supplementary Table 7, see <http://ajp.amjpathol.org>), confirming at the protein level the RNA expression of these two important virulence genes.

Carbohydrate and Energy Metabolism

Contiguous coding regions (M5005_spy1062-7) involved in the transport and catabolism of complex carbohydrates known as maltodextrins were among the highest-expressed GAS transcripts detected in our *in vivo* data (Supplementary Table 3, see <http://ajp.amjpathol.org>). The corresponding genes encode a maltose/maltodextrin utilization protein (MalA); a maltodextrin ATP-binding cassette transport system (MalC and MalD); two enzymes involved in maltodextrin rearrangement (cyclomaltodextrin glucanotransferase AmyA and cyclomaltodextrinase AmyB), and a maltose/maltodextrin solute-binding

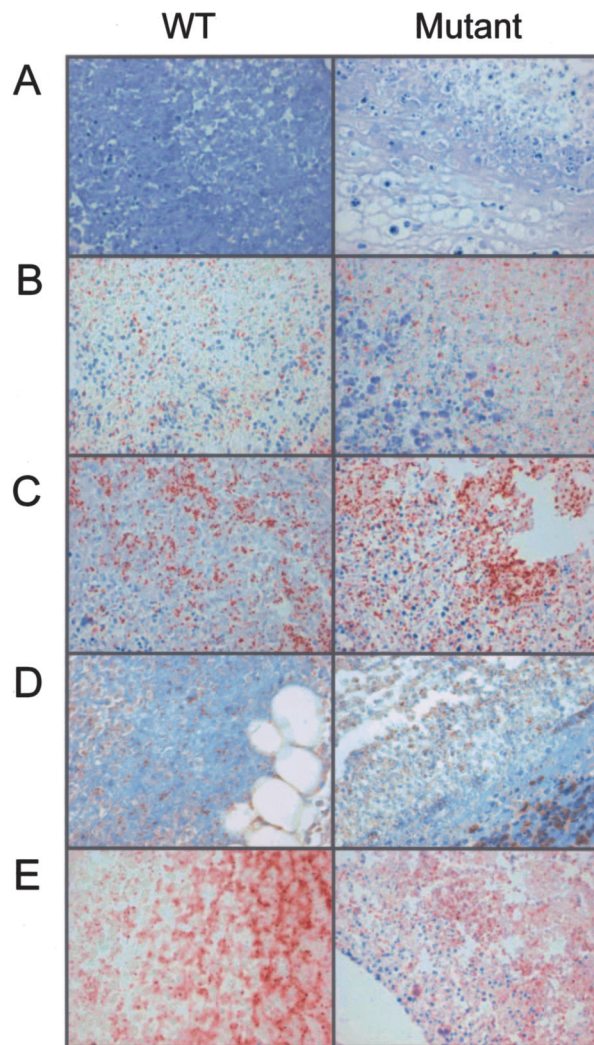


Figure 5. Immunohistochemical confirmation of GAS protein expression during soft tissue infection. Representative IHC results for tissue obtained from mice infected with GAS WT MGAS5005 (left) and $\Delta covR$ mutant strain JRS950 (right) analyzed with anti-M3.1/1-24 antibodies (negative control) (A); anti-SPE A2; M5005_spy0996 (B); anti-MalE; M5005_spy 1058 (C); anti-Obp; M5005_spy1308 (D); and anti-SIC; M5005_spy1718 rabbit polyclonal antisera (E) at 2 days after inoculation.

protein (MalX), respectively. Synchronous with these results, low transcript levels were detected for two nearby genes encoding putative transcriptional repressors, the maltose operon regulator MalR (M5005_spy1057) and an inferred LacI-family regulator (designated herein as MalT; M5005_spy1061), suggesting a cause and effect relationship. Functionally related transcripts (M5005_spy1055-60) also were detected adjacent to chromosome region (M5005_spy1062-7), including genes encoding enzymes maltodextrin phosphorylase (MalP/GlgP) and amylomaltase (MalQ/MalM), and a maltose/maltosaccharide/maltodextrin-binding ATP-binding cassette transport system (MalEFG). Our analysis of coordinated expression of transcripts discovered another functionally related locus nearby (M5005_spy1680-2), that encoded the Mga-activated polysaccharidase designated pullulanase⁴⁷; a dextran glucosidase, and a maltose/maltodextrin solute-binding protein

MsmK, suggesting that maltodextrin-related transcript co-expression is likely important in GAS soft tissue infection.

Recent published findings suggested that transcripts involved in maltodextrin metabolism (M5005_spy1061-7) may be positively regulated by the TCS designated SptR/S loci (M5005_Spy0680/1).⁴⁸ However, we found no correlation of *malT-malX* expression with either *sptR* or *sptS* transcripts ($r < 0.5$), whereas positive correlations were revealed with transcripts encoding the TCS designated LytR/S, whose homologs affect cell wall metabolism in *Staphylococcus aureus*⁴⁹ ($r > 0.7$; Supplementary Table 4, see <http://ajp.amjpathol.org>). Strong correlation with *lytRS* ($r > 0.85$) was similarly observed for the chromosomal region flanking *lytRS* (M5005_Spy1303-10), which coincidentally encodes yet another putative complex sugar transport system. Together, these findings provide supporting evidence for involvement of the CovR-regulated LytR/S TCS in mediating GAS complex carbohydrate metabolism during soft tissue infection.

GAS ferments carbohydrates via the Embden-Meyerhof-Parnas (EMP) pathway to form pyruvate for energy metabolism. As with many bacteria, glucose is the preferred catabolic substrate and high glucose concentrations repress expression of alternative catabolic pathways via the catabolite repressor CcpA.⁵⁰ We discovered that *ccpA* was expressed at low range (ranked 342nd) in the mouse tissues suggesting that glucose supplies were limiting at that time. In agreement with this finding, high levels of lactate oxidase (*lctO*; ranked 63rd) transcripts, of which the protein product is known to convert lactate to acetate thereby generating ATP via acetyl phosphate,⁵¹ were detected simultaneously (Supplementary Table 3, see <http://ajp.amjpathol.org>). Together, these results suggest a glucose-poor environment with adaptation by GAS for using lactate as a carbon energy source during soft tissue infection. Elevated transcripts also were detected for *pfl* and *pta* encoding pyruvate formate-lyase and phosphotransacetylase (ranked 81st and 102nd, respectively), which are involved in pyruvate oxidation to coenzyme A and formate⁵¹ suggesting that metabolic pathways downstream of pyruvate were activated. However, GAS also is capable of fermenting nitrogen-containing compounds for energy metabolism generating 1 mol of ATP per mol of arginine or histidine metabolized and high levels of transcripts were detected for the histidine catabolic pathway and histidine deaminase (*hutH*; ranked 90th), which generates urocanate and ammonia. Coordinate with histidine catabolic pathway expression, a polycistronic transcript (M5005_Spy1270-5) encoding arginine deiminase (ADI; ranked 177th) along with transcripts encoding other related functions within the arginine catabolic pathway (Supplementary Table 3, see <http://ajp.amjpathol.org>) were detected.

GAS Transcripts Correlated with Gross Cutaneous Injury

Analysis of WT-inoculated tissue array data revealed 18 GAS transcripts whose expression correlated directly with lesion volume ($Q < 0.05$; Supplementary Table 8,

see <http://ajp.amjpathol.org>). Of these, six encode genes of unknown function, whereas seven are localized in the bacterial cytoplasm and involved in information processing, including transcriptional repressor ArgR1 (M5005_Spy1229; ranked 313th), the multigene transcriptional activator Mga (ranked 418th), and the DNA mismatch repair protein MutL (ranked 592nd). No GAS transcripts exhibited significant correlation with erythema volume ($Q > 0.05$; data not shown).

Discussion

Bacterial pathogens use coordinated gene expression to respond to environmental change and to elude host defenses, thereby facilitating persistence, proliferation, invasion, and dissemination. As GAS infects humans using a variety of different routes (skin, mucosal surfaces, and blood), it likely expresses distinct sets of genes that enable it to adapt to each diverse and changing host microenvironment.¹¹ Current understanding of bacterial gene regulation is based primarily on studies conducted under controlled laboratory conditions, in which typically only one variable is altered at a time. Although this approach is powerful in pathogenesis studies, it does not adequately mimic the extensive variety of signals experienced simultaneously when bacteria are growing in the host.¹² Global expression microarray (transcriptome) analysis of bacteria grown *in vivo* provides a unique opportunity to identify how pathogens adjust gene expression genome-wide in response to complex host environments.¹⁰

Abundant GAS Transcripts in Soft Tissue Infection

WT GAS is a superbly adapted pathogen, able to protect itself against damaging host effectors during murine soft tissue infection by expressing numerous anti-oxidant, molecular chaperone, cytotoxin, and cell wall/lipoteichoic acid modifying proteins. For example, we observed *emm* transcript-encoding M protein, the hypervariable major surface antigen used for serological typing of GAS strains, predominate in lesions. This well-studied bacterial virulence determinant acts as an adhesin; promotes inflammation; impedes phagocytosis by binding complement control factors, fibrinogen, kininogen, and also plasminogen;^{3,4} and is abundantly transcribed during GAS culture *ex vivo* in blood.²⁰ Host fibrinogen levels rise sharply during tissue inflammation and injury, and M protein/fibrinogen complexes activate PMNs through β 2-crosslinking triggering release of heparin-binding protein (HBP), a proinflammatory mediator which in turn promotes excessive vascular leakage.⁵² Another important molecule whose RNA was present in high amounts in our tissue model was GAS cysteine protease SpeB, which has been shown to cleave many host proteins including cytokine precursors, cell receptors, fibrin, vitronectin, matrix proteoglycans, cationic antimicrobial peptides, and immunoglobulins, thereby contributing to endothelial and epidermal damage, tissue destruction, and bacterial

dissemination.⁵³⁻⁵⁵ SpeB enzymatic activity also releases fragments of fibrinogen-complexed M1 protein [fibrinogen-M1], thereby contributing to vascular leakage and host tissue damage.⁵² However, at the same time, we detected virtually no *grab* transcripts, which encode a host protease inhibitor α_2 -macroglobulin-binding bacterial surface protein designated GRAB. α_2 -Macroglobulin-GRAB complexes concentrate SpeB activity at the bacterial surface and against smaller substrates, thereby protecting GAS against killing by the antibacterial peptide LL-37.⁵⁶ Because SpeB also degrades many GAS extracellular proteins in the absence of GRAB, not surprisingly we detected modulated, mid-ranging *speB* transcripts (ranked 304th in WT) at 7- to 25-fold lower levels than the most abundantly detected GAS transcripts in tissues. Therefore, in the soft tissue model we propose that low levels of *grab*, moderate levels of *speB*, and high *emm1.0* transcript production occurs, providing sufficient SpeB proteolytic activity and hence M1-fibrinogen complex formation all of which leads to substantial tissue damage. Increasing transcription of *speB* throughout time during soft tissue infection has recently been described.¹¹ These observations, coupled with postinfectious induction of tissue edema, which leads to depletion of vascular volume, may account for the rapid onset of life-threatening hypotension and shock in severe GAS infections.⁷ Interruption of this pathophysiological pathway could be critical for therapeutic intervention of aggressive, invasive GAS infections.

During soft tissue infection, WT GAS expresses high levels of transcripts for products that inhibit host innate defenses and protect GAS against neutrophil-derived reactive oxygen species and antimicrobial peptides. For example, *sic* (ranked first) and *spd* (ranked 14th) were among the most abundantly expressed GAS transcripts measured. We confirmed the high expression levels of SIC by IHC analysis of infected tissues (Figure 4). SIC is known to inhibit complement-mediated bacterial lysis via C5b67 binding, innate defenses such as lysozyme and PMNs, and can eliminate chemotactic recruitment of leukocytes, T cells, and mast cells by inactivating antimicrobial peptides such as LL-37 and β -defensins.^{57,58} Similar findings were observed *in vivo* in nonhuman primates and after GAS culture *ex vivo* in whole blood where Mga regulon transcripts were the highest expressed of all detected regulons.^{10,20} On the other hand, streptodornase (*spd*) is a secreted DNase that may interfere with PMN function, by degradation of innate immune structures known as neutrophil extracellular traps.^{17,59} In addition, high levels of expression of *sagA* (ranked 28th), which encodes the potent cytolytic SLS, was notable because SLS is thought to accelerate necrotic fascial injury through cytotoxic or apoptotic effects on many cell types including, but not limited to, neutrophils.⁶⁰ The untranslated mRNA of the pleiotropic effect locus (*pel*), which incidentally contains *sagA*, also acts as an anti-sense RNA transcriptional regulator, augmenting GAS virulence factor expression [SIC, M-protein, extracellular NAD-glycohydrolase (NADase encoded by *nga/spn*), plasminogen activator streptokinase encoded by *ska*, and SpeB] when *pel* RNA expression is induced.^{61,62} We

detected abundant *sagA* transcripts; thus *pel*-induced virulence gene expression may be predicted, as was observed in this study for all but *nga* (ranked 780th in WT extracts). Therefore, these results, when coupled with the elevated expression of the neutrophil chemoattractant (interleukin-8)-cleaving SpyCEP protease (ranked 97th),³⁰ support the idea that coordinated, increased expression of *sic*, *spd*, *sagA*, *speB*, and *spyCEP* likely accounts for lack of inflammatory cells present at GAS sites in deep tissues.⁶³ Expression of the aforementioned GAS products, along with M1 protein, streptokinase, and the host cytolytic streptolysin O (SLO; ranked 268th) and NADase likely contributes to much of the cutaneous and subcutaneous pathologies observed in our animal model tissue infections (Supplementary Table 3; reviewed in Supplementary Table 9,⁶⁴⁻⁸⁴ see <http://ajp.amjpathol.org>).

Serotype M1 strains are often associated with postinfectious sequelae, possibly resulting from immunological cross-reactivity of GAS antigens with host tissues.^{3,4} Virtaneva and colleagues,¹⁰ observed during nonhuman primate experimental pharyngitis, high *in vivo* levels of GAS transcripts, such as *emm*, cardiolipin synthetase, and myosin-cross reactive streptococcal antigen, results we have now confirmed in our *in vivo* study; M protein (*emm*, ranked seventh), hydroxylated phospholipid cardiolipin synthetase (CL synthase, M5005_Spy0926; ranked 111th), and 67-kd myosin-crossreactive streptococcal antigen⁸⁵ (M5005_Spy0385, ranked 125th). Increased production of these transcripts in both the oropharynx model and now the soft-tissue model suggests an increased risk of nonsuppurative sequelae, a prospect that warrants further study.

Three proteins encoded by up-regulated WT transcripts; *gap/plr*, *eno*, and *ska*, ranked 71st, 117th, and 453rd, respectively, are known to interact or bind with host plasminogen.³ Fibrinogen binding to M-protein (*emm*) leads to host plasminogen binding. Bound plasminogen interacts with GAS streptokinase to generate a bacterial-bound, serine protease-designated plasmin.⁸⁶ GAS surface-localized plasmin has been implicated in GAS dissemination.^{3,41,74-86} Statistically higher expression of *ska* transcripts in the $\Delta covR$ mutant likely contributed to lesion size differences between mutant and WT. Our observation of abundant *plr* transcripts is also noteworthy given that the encoded protein also has been identified as an acute poststreptococcal glomerulonephritis-associated antigen (designated NAP1r).^{87,88}

GAS is sensitive to penicillin *in vitro*, yet high-dose penicillin demonstrates reduced bactericidal activity *in vivo*, attributable in part to inadequate drug perfusion in poorly vascularized or necrotic fascia.⁸⁹ In addition, large GAS inocula refractory to penicillin have been suggested as metabolically inactive or demonstrating decreased presence of penicillin-binding proteins (PBPs).^{7,90,91} At the time point of our collected tissue samples, we detected abundant levels of PBP1A- and PBP2A-encoding transcripts and found no evidence suggesting inactive or reduced metabolic activity *in vivo*. Previously published studies have demonstrated that our custom high-density array approach is capable of sensitive detection of low

copy transcripts.¹⁰ Therefore, the mechanisms responsible for reduced efficacy of penicillin treatment *in vivo* may be more complex than previously thought, perhaps warranting focused study. Although we observed abundant GAS transcripts encoding proinflammatory M protein, SLS cytotoxin, and plasmin receptor Plr (ranked seventh, 28th, and 71st, respectively), decreased protein expression encoded by these genes may explain why co-administration of clindamycin (a protein synthesis inhibitor) seems to enhance bacterial clearance in progressive cases, relative to penicillin treatment alone.^{4,89} Future investigations are warranted to elucidate this clindamycin phenomenon.

Transcripts encoding GAS PTSAg exotoxins were virtually undetectable at the time of our tissue sampling. PTSAGs are potent T-cell mitogens that stimulate a massive release of inflammatory cytokines and that correlate with severity of systemic clinical manifestations in GAS infections.⁹² However, data observed in nonhuman primates suggest that PTSAGs SpeA2, SpeJ, and SmeZ demonstrate differential expression before, during, and after pharyngeal colonization.¹⁰ Our findings therefore support clinical and experimental data revealing reciprocal, or temporal expression of SpeA and SpeB *in vivo*.⁹³ Recent observations suggest that direct contact with human PBMCs, which occurs early in infection, induces SpeA expression⁹⁴ whereas cysteine protease SpeB expression increases temporally during later stages of soft tissue infections.¹¹ Our *in situ* immunohistochemical data showed immunoreactivity for SpeA at 48 hours after inoculation. Numerous GAS proteins are known to contribute to the induction of neutrophil apoptosis,⁶⁹ leading to an absence of proinflammatory cells at GAS sites in deep tissues.⁶³ Together, these findings do not preclude the expression of PTSAg exotoxins at early stages of soft tissue infection, but rather suggest that the time we harvested the tissue (2.5 days after infection) was more likely a mid point during the GAS soft tissue infection time course.

Adaptive Metabolism

Central and adaptive metabolism profoundly affects pathogen persistence *in vivo* and likely accounts for why GAS regulatory- and metabolism-associated transcripts (primarily cytoplasmic) predominate in soft tissues. We found that *in vivo* GAS abundantly transcribes genes in two chromosomal regions (M5005_spy1062-7 and 1680-2), which are involved in metabolizing complex carbohydrates such as maltodextrins, which may include but not be limited to glycogen, maltotetraose, maltotriose, and maltose. These expression results are consistent with a report in which 81% of convalescent-phase sera from patients with invasive GAS infections had antibodies reactive with M5005_SPy1680, also known as pullulanase (PulA).⁹⁵ PulA is a polysaccharidase that is positively regulated by the multigene transcriptional activator called Mga and which uses host glycoproteins as its enzymatic substrate.⁴⁷ GAS metabolism of complex host-derived carbohydrates may be particularly important dur-

ing soft tissue infections because of abundant host glycoproteins and host cell contents released during cell lysis. Degradation of host proteins in necrotic fascia may contribute to fermentation of arginine and histidine during soft tissue infection. In turn, fermentation of amino acids produces ammonia, which could beneficially neutralize surrounding pH thereby protecting GAS from acid-induced damage.⁹⁶ GAS arginine deaminase activity has been linked to inhibition of human peripheral blood mononuclear cell proliferation.⁹⁷ The arginine deiminase system of *Streptococcus suis* is induced by arginine, elevated temperature, and reduced oxygen tension, and is subject to carbon catabolite repression.⁹⁸ Therefore, low glucose and hypoxic microenvironments, after vascular injury, may serve as signals that trigger the GAS adaptive response, which in turn enables bacterial persistence and proliferation in soft tissues.

GAS Transcript Expression Is Not Correlated with Cutaneous Injury

Correlation analysis of GAS transcripts with cutaneous lesion volume produced only a few candidates ($n = 18$), most of which appear to encode proteins predicted to be cytoplasmic or membrane-bound in function. Although these discoveries are attractive, lack of biochemical functional annotation for these genes limits our ability to hypothesize their role in lesion development. These findings are consistent with the clinical observation that substantial necrosis occurs subcutaneously in some human infections without overt injury of the overlying skin.¹³ Further studies are needed to identify bacterial genes associated with soft tissue disease severity and the functions they may impart in this important aspect of disease.

GAS Strain Comparison in Vivo

The CovR response regulator has been shown to play a central role in GAS regulatory networks by directly or indirectly influencing expression of 15% of all GAS chromosomal genes during *in vitro* growth.¹⁴ CovR negatively regulates biosynthesis of the anti-phagocytic hyaluronic acid capsule⁴² and the expression of numerous cell-surface-associated and secreted proteins known to promote survival or impart virulence in humans.^{14,42-44} Hyperencapsulated GAS variants with spontaneous *covR/S* mutations have been isolated after WT bacterial passage in human blood, passage in mice, or after natural-acquired human infections.⁹⁹⁻¹⁰¹ Importantly, high GAS bacterial colony-forming unit numbers has been found to negatively correlate with *covR* expression *in vivo* during acute phase GAS pharyngitis in primates.¹⁰ Despite absence of CovR function in the mutant strain, we found fewer differentially expressed transcripts ($n = 76$) between mutant and WT during soft tissue infection than we had extrapolated from our previous *in vitro* studies.^{14,20} This led us to hypothesize that transcription of *covR* in WT GAS occurs at lower levels *in vivo* during soft tissue infection

at the time point studied than under *in vitro* growth conditions. Indeed, *covR* and *covS* transcripts ranked 269th and 755th, respectively, in GAS-infected lesion extracts, whereas *covR/covS* transcripts were more abundant (transcripts ranked 30th to 280th) during a 90-minute time course of culturing in human blood *ex vivo*.²⁰ This finding supports *in vivo* down-regulation of *covR* expression,^{10,99–101} leading to increased virulence factor production¹⁴ and resultant tissue pathology and suggests that soft tissue effectors not present in whole blood are likely responsible for this down-regulation. Based on *in vitro* studies, high [Mg²⁺] concentration has been proposed as an environmental stimulus responsible for up-regulation of *CovR/S* expression and therefore repression of the expression of *CovR*-regulated genes.¹⁰² *In vivo* microenvironment analysis of magnesium concentrations throughout time, during the course of soft tissue infections may provide insight into the effectors regulating *CovR/S* expression.

In contrast to *in vitro* findings,^{14,20} more than half of the total number of transcripts functionally related to stress adaptation were transcribed at lower levels *in vivo* in the Δ *covR* mutant as compared with the WT. Given that we detected more transcripts encoding the transcriptional repressor of class I stress genes (designated HrcA)³³ in WT (ranked 15th) than in mutant (ranked 42nd), we would predict the converse; that transcript levels encoding the negatively regulated class I molecular chaperones (DnaJ, DnaK, and GroES) and chaperone proteases (GroEL, ClpP, and ClpL) would be higher in Δ *covR*-infected tissues as compared with WT extracts. These results imply other peripheral regulatory mechanisms may be in place, and suggest that less stress adaptation may be required in the localized environment when host cell damaging virulence factors are derepressed. This finding serves to highlight the importance of conducting *in vivo* analyses to improve understanding of pathogen-host interactions.¹²

Emerging Model of GAS Gene Regulation in Vivo

Our study has provided the first *in vivo* analysis of GAS gene expression during soft tissue infection. By differential gene expression, GAS successfully transitions through three stages of host infection: namely, 1) establishment of infection, 2) adaptation, and 3) dissemination (Figure 6). Information about stage 1 is based on an expanding body of work,^{8,10,11,34,103} and our results support this information by combined early expression of *Mga*, *Ihk/Irr*, and *FasBCA/X* regulatory systems that promote evasion of immune and innate host defenses and enhance host cell contact through surface adhesin production. Down-regulation of the negative regulatory systems of *PerR*, *CovR/S*, and *CrgR* promote production of reactive oxygen species detoxifying enzymes, hyaluronic acid capsule, and antimicrobial peptide resistance mechanisms, respectively,^{8,35,103–107} and our soft tissue model demonstrates similar results. Interestingly, we

have discovered that transcription of transport and central metabolism genes appears tailored to unique GAS environments where host glycopeptides and complex carbohydrates are available, including maltodextrins, but which must be used under acidic and hypoxic conditions. Alteration of these conditions ultimately enables GAS to persist and proliferate. GAS cell wall modifications can reduce cell permeability and thereby increases antimicrobial peptide resistance.¹⁰⁸ The reduced efficacy of penicillin-based antibiotics in treating circulation-poor deep-seated GAS infections also may be related to this GAS adaptation. Throughout time, production and accumulation of the SLS cytolysin, *SpeB* cysteine protease, proinflammatory PTSAGs, and fibrinogen-M1 protein complexes have the ability to cause cumulative damage to host cells, resulting in disruption of host barriers leading to bacterial dissemination. Evidence suggests that dissemination of GAS from localized tissues, occurs as GAS undergoes additional remodeling, which can include late-stage cysteine protease expression,¹¹ (Figure 6). A carbon catabolite response element (*cre*) operator site precedes the *Mga* promoter, and thus expression of *Mga* (and virulence factors it transcriptionally activates) may be subject to carbon catabolite control.¹⁰⁹ Linkage of the *Mga* regulon to GAS nutritional requirements may help explain why in our study we observed correlated expression between *eno* encoding glycolytic and surface α -enolase and *emm* encoding M1 protein. The linkage of GAS metabolism regulation and virulence factor expression to nutritional signals provides an intuitive model that helps explain GAS movement from chronic or acute sites to naïve sites.

Few studies to date have succeeded in measuring global transcription in the *in vivo* host environment.^{10,110–113} This study has overcome difficult technical hurdles to provide a unique dataset on the GAS transcriptome during soft tissue infection. Twenty to thirty percent of many pathogen genome ORFs lack biochemical functional annotation. Our transcriptome data suggest that many of these hypothetical ORFs of unknown function are expressed in the soft tissue model, often with good correlation to other virulence factors and pathology. Our data provides new avenues of study for determining the role of these hypotheticals and whether diagnostic or vaccine candidates exist within this group of genes. Owing to the fact that bacterial sampling required animal sacrifice, our end-point study probed mid and late stages of infection (stages 2 and 3, Figure 6). The proportion of adapting versus disseminating bacteria in the tissue extracts cannot be known and thus, the transcriptomes obtained represent averages for the bacterial population. Future studies will involve optimization and protocol development for sensitive array analysis of microscopic tissue biopsies collected throughout time after low-dose intradermal inoculation. These experiments will provide a GAS transcriptome profile of the temporal natural history of soft tissue infection. In addition, we anticipate future tissue model studies will also focus on the comparison of *in vivo* GAS transcriptomes of epidemiologically distinct strains. Last, although our infection model mimics conditions present in infected humans, we acknowledge that mice cannot adequately replicate either the highly complex environment that

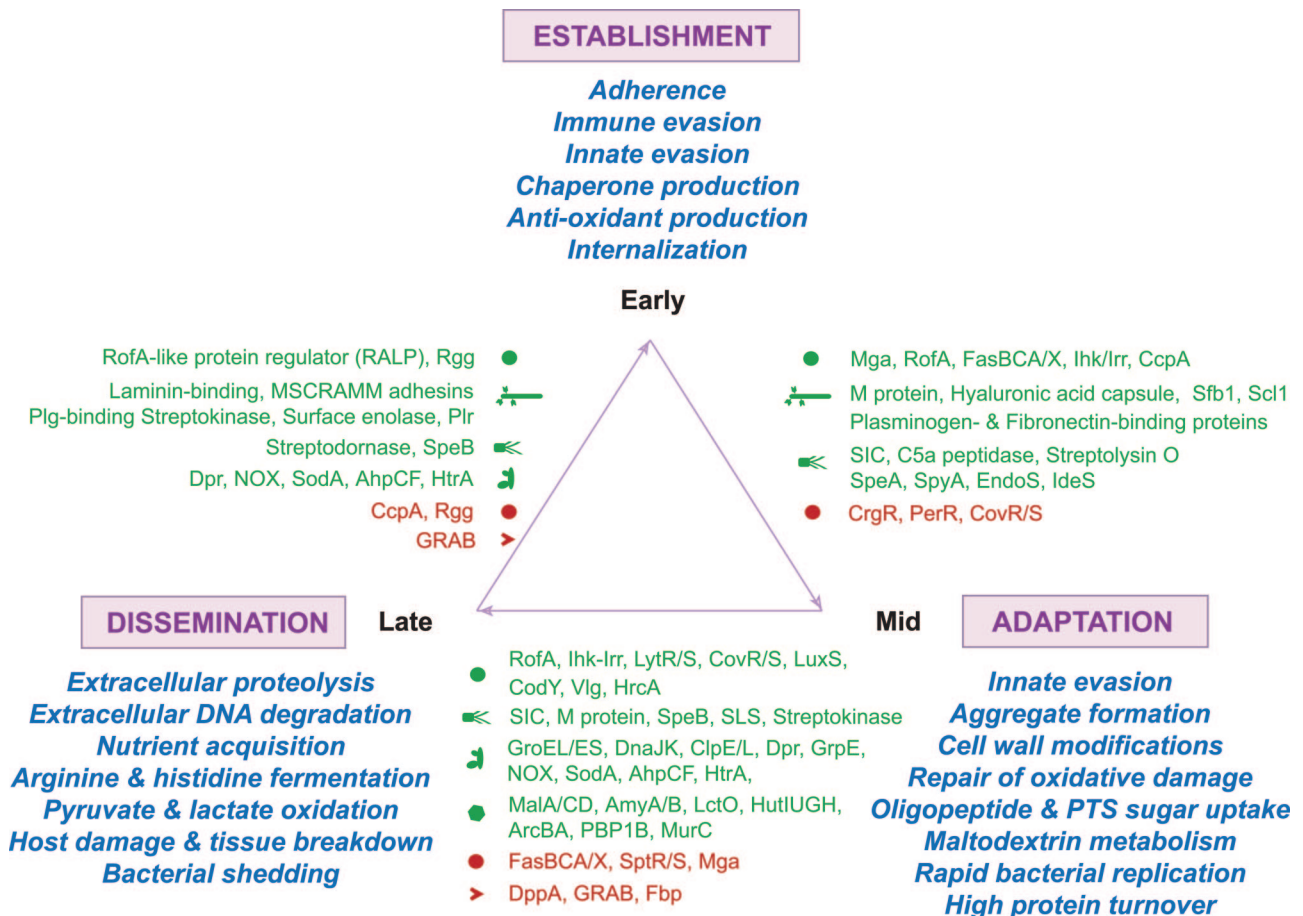


Figure 6. Emerging model of GAS gene regulation in soft tissue infection. Depicted schematically is the emerging model of GAS gene expression *in vivo* during suppurative infections. By finely modulating gene expression, GAS transitions through three general stages during host infection: namely, 1) establishment (top), 2) adaptation (bottom right), and 3) dissemination (bottom left). Establishment is achieved through bacterial adhesin production and evasion of immune and innate host defenses. Proliferation in large bacterial aggregates provides enhanced opportunity for bacterial resistance and concentration of extracellular products aimed at disrupting various host functions. Adaptive expression of nutrient transport and central metabolism systems enables GAS to acquire and use host peptides and complex carbohydrate substrates, such as maltodextrins. Cumulative damage to host cells, tissue injury, and disruption of host barriers results in enhanced potential for bacterial dissemination to naïve host sites. GAS undergoes additional transcription changes that promote persistence elsewhere, initiating new foci of infection. Green text (up-regulation); red text (down-regulation).

GAS encounters in the infected human host or the human host response. Future bacterial expression studies should also be performed during natural human infections, provided appropriate precautions are taken to minimize technical variation and to adequately account for patient-to-patient variability associated with the nature and logistics of clinical specimen sampling, which often occurs under life-saving and time-constrained circumstances involving patients recently treated with antimicrobial agents. Correlation analysis will help pinpoint those GAS genes or ORFs expressed in common during different stages of disease, which may lead to novel, broad-spectrum therapeutic, vaccine, or diagnostic candidates against this important human pathogen.

Concluding Statement

A full understanding of host/pathogen interactions requires knowledge of gene expression *in vivo*.^{10, 12, 114–116} Our data provide new information about GAS gene expression during soft tissue infection, and highlight the

benefit of using sensitive high-density microarray analysis. The *in vivo*, soft tissue GAS transcriptome differs significantly from that obtained in blood *ex vivo*,²⁰ in isolated cell populations,³⁵ and during colonization and acute pharyngitis,¹⁰ stressing the ability of GAS to alter its transcriptome to permit growth in the different host environments. Our results unambiguously demonstrate that many proven and putative GAS virulence factors are transcribed *in vivo* and contribute to extensive cellular pathology observed in GAS soft tissue infections. Our study provides the first genome-wide view of the GAS transcriptome, *in vivo*, during skin infection and suggests numerous avenues for investigation into targeted therapeutics against this important human pathogen. This analysis framework is cross-applicable for examining other pathogens causing invasive infections.

Acknowledgments

We thank J. Yang and R. Lempicki of the Science Application International Corporation-Frederick Affymetrix

core facility for hybridizations; R. Larson and J. Kupko (Rocky Mountain Laboratories) for providing technical expertise with animal handling and database submission, respectively; T.J. Downey and S. Jing (Partek, Inc.) and E. Spitznagel (University of Washington) for statistical assistance; J.R. Scott (Emory School of Medicine) for providing the $\Delta covR$ mutant derivative of MGAS5005 (strain JRS950); P. Schlievert (University of Minnesota) for anti-SpeA antibody; and G. McClarty and T.G. Schwan for critical review of the manuscript.

References

1. DiNubile MJ, Lipsky BA: Complicated infections of skin and skin structures: when the infection is more than skin deep. *J Antimicrob Chemother* 2004, 53:37–50
2. Musser JM, Krause RM: The revival of group A streptococcal diseases, with a commentary on staphylococcal toxic shock syndrome. *Emerging Infections*. Edited by Krause RM. New York, Academic Press, 1998, pp 185–218
3. Cunningham MW: Pathogenesis of group A streptococcal infections. *Clin Microbiol Rev* 2000, 13:470–511
4. Bisno AL, Brito MO, Collins CM: Molecular basis of group A streptococcal virulence. *Lancet Infect Dis* 2003, 3:191–200
5. O'Brien KL, Beall B, Barrett NL, Cieslak PR, Reingold A, Farley MM, Danila R, Zell ER, Facklam R, Schwartz B, Schuchat A: Epidemiology of invasive group A Streptococcus disease in the United States, 1995–1999. *Clin Infect Dis* 2002, 35:268–276
6. Stevens DL: The flesh-eating bacterium: what's next? *J Infect Dis* 1999, 179:S366–S374
7. Stevens D: Streptococcal toxic shock syndrome associated with necrotizing fasciitis. *Annu Rev Med* 2000, 51:271–288
8. Kreikemeyer B, Mclver KS, Podbielski A: Virulence factor regulation and regulatory networks in *Streptococcus pyogenes* and their impact on pathogen-host interactions. *Trends Microbiol* 2003, 11:224–232
9. Hynes W: Virulence factors of the group A streptococci and genes that regulate their expression. *Front Biosci* 2004, 9:3399–3433
10. Virtaneva K, Porcella SF, Graham MR, Gardner DJ, Bailey JR, Parnell MJ, Musser JM: Longitudinal analysis of group Streptococcus transcriptome in experimental pharyngitis in cynomolgus macaques. *Proc Natl Acad Sci USA* 2005, 102:9014–9019
11. Loughman JA, Caparon M: Regulation of SpeB in *Streptococcus pyogenes* by pH and NaCl: a model for in vivo gene expression. *J Bacteriol* 2006, 188:399–408
12. Handfield M, Progulske-Fox A, Hillman J: In vivo induced genes in human diseases. *Periodontol* 2000 2005, 38:123–134
13. Headley AJ: Necrotizing soft tissue infections: a primary care review. *Am Fam Physician* 2003, 68:323–328
14. Graham MR, Smoot LM, Migliaccio CAL, Virtaneva K, Sturdevant DE, Porcella SF, Federle MJ, Adams GJ, Scott JR, Musser JM: Virulence control in group A Streptococcus by a two-component gene regulatory system: global expression profiling and in vivo infection modeling. *Proc Natl Acad Sci USA* 2002, 99:13855–13860
15. Hoe NP, Nakashima K, Lukomski S, Grigsby D, Liu M, Kordari P, Dou SJ, Pan X, Vuopio-Varkila J, Salmelinn S, McGeer A, Low DE, Schwartz B, Schuchat A, Naidich S, De Lorenzo D, Fu YX, Musser JM: Rapid selection of complement-inhibiting protein variants in group A Streptococcus epidemic waves. *Nat Med* 1999, 5:924–929
16. Sumbly P, Porcella SF, Madrigal AG, Barbian KD, Virtaneva K, Ricklefs SM, Sturdevant DE, Graham MR, Vuopio-Varkila J, Hoe NP, Musser JM: Evolutionary origin and emergence of a highly successful clone of serotype M1 group A Streptococcus involved multiple horizontal gene transfer events. *J Infect Dis* 2005, 192:771–782
17. Sumbly P, Barbian KD, Gardner DJ, Whitney AR, Welty DM, Long RD, Bailey JR, Parnell MJ, Hoe NP, Adams GG, DeLeo FR, Musser JM: Extracellular deoxyribonuclease made by group A Streptococcus assists pathogenesis by enhancing evasion of the innate immune response. *Proc Natl Acad Sci USA* 2005, 102:1679–1684
18. Lukomski S, Hoe NP, Abdi I, Rurangirwa J, Kordari P, Liu M, Dou SJ, Adams GG, Musser JM: Nonpolar inactivation of the hypervariable streptococcal inhibitor of complement gene (sic) in serotype M1 *Streptococcus pyogenes* significantly decreases mouse mucosal colonization. *Infect Immun* 2000, 68:535–542
19. Lukomski S, Montgomery CA, Rurangirwa J, Geske RS, Barrish JP, Adams GJ, Musser JM: Extracellular cysteine protease produced by *Streptococcus pyogenes* participates in the pathogenesis of invasive skin infection and dissemination in mice. *Infect Immun* 1999, 67:1779–1788
20. Graham MR, Virtaneva K, Porcella SF, Barry WT, Gowen BB, Johnson CR, Wright FA, Musser JM: Group A Streptococcus transcriptome dynamics during growth in human blood reveals bacterial adaptive and survival strategies. *Am J Pathol* 2005, 166:455–465
21. Alm EJ, Huang KH, Price MN, Koche RP, Keller K, Dubchak IL, Arkin AP: The MicrobesOnline web site for comparative genomics. *Genome Res* 2005, 15:1015–1022
22. Li C, Wong WH: Model-based analysis of oligonucleotide arrays: expression index computation and outlier detection. *Proc Natl Acad Sci USA* 2001, 98:31–36
23. Yoon H, Liyanarachchi S, Wright FA, Davuluri R, Lockman JC, de la Chapelle A, Pellegata NS: Gene expression profiling of isogenic cells with different TP53 gene dosage reveals numerous genes that are affected by TP53 dosage and identifies CSPG2 as a direct target of p53. *Proc Natl Acad Sci USA* 2002, 99:15632–15637
24. Storey JD, Tibshirani R: Statistical significance for genomewide studies. *Proc Natl Acad Sci USA* 2003, 100:9440–9445
25. Yekutieli D, Benjamini Y: Resampling based FDR controlling multiple hypotheses testing. *J Stat Plan Infer* 1999, 82:171–196
26. Barry WT, Nobel AB, Wright FA: Significance analysis of functional categories in gene expression studies: a structured permutation approach. *Bioinformatics* 2005, 21:1943–1949
27. Lei B, Liu M, Chesney GL, Musser JM: Identification of new candidate vaccine antigens made by *Streptococcus pyogenes*: purification and characterization of 16 putative extracellular lipoproteins. *J Infect Dis* 2004, 189:79–89
28. Salim KY, Cvitkovitch DG, Chang P, Bast DJ, Handfield M, Hillman JD, de Azavedo JCS: Identification of group A Streptococcus antigenic determinants upregulated in vivo. *Infect Immun* 2005, 73:6026–6038
29. Teng F, Nannini EC, Murray BE: Importance of gls24 in virulence and stress response of *Enterococcus faecalis* and use of the Gls24 protein as a possible immunotherapy target. *J Infect Dis* 2005, 191:472–480
30. Edwards RJ, Taylor GW, Ferguson M, Murray S, Rendell N, Wrigley A, Bai Z, Boyle J, Finney SJ, Jones A, Russell HH, Turner C, Cohen J, Faulkner L, Sriskandan S: Specific C-terminal cleavage and inactivation of interleukin-8 by invasive disease isolates of *Streptococcus pyogenes*. *J Infect Dis* 2005, 192:783–790
31. Terao Y, Kawabata S, Kunitomo E, Nakagawa I, Hamada S: Novel laminin-binding protein of *Streptococcus pyogenes*, Lbp, is involved in adhesion to epithelial cells. *Infect Immun* 2002, 70:993–997
32. Coye LH, Collins CM: Identification of SpyA, a novel ADP-ribosyltransferase of *Streptococcus pyogenes*. *Mol Microbiol* 2004, 54:89–98
33. Woodbury R, Haldenwang WG: HrcA is a negative regulator of the dnaK and groESL operons of *Streptococcus pyogenes*. *Biochem Biophys Res Commun* 2003, 302:722–727
34. Ricci S, Janulczyk R, Bjorck L: The regulator PerR is involved in oxidative stress response and iron homeostasis and is necessary for full virulence of *Streptococcus pyogenes*. *Infect Immun* 2002, 70:4968–4976
35. Voyich JM, Braughton KR, Sturdevant DE, Vuong C, Kobayashi SD, Porcella SF, Otto M, Musser JM, DeLeo FR: Engagement of the pathogen survival response used by group A Streptococcus to avert destruction by innate host defense. *J Immunol* 2004, 173:1194–1201
36. Janulczyk R, Ricci S, Bjorck L: MtsABC is important for manganese and iron transport, oxidative stress resistance, and virulence of *Streptococcus pyogenes*. *Infect Immun* 2003, 71:2656–2664
37. King KY, Horenstein JA, Caparon MG: Aerotolerance and peroxide resistance in peroxidase and perR mutants of *Streptococcus pyogenes*. *J Bacteriol* 2000, 182:5290–5299
38. Gibson CM, Mallett TC, Claiborne A, Caparon MG: Contribution of

- NADH oxidase to aerobic metabolism of *Streptococcus pyogenes*. *J Bacteriol* 2000, 182:448–455
39. Yamamoto Y, Fukui K, Koujin N, Ohya H, Kimura K, Kamio Y: Regulation of the intracellular free iron pool by Dpr provides oxygen tolerance to *Streptococcus mutans*. *J Bacteriol* 2004, 186:5997–6002
 40. Ibrahim YM, Kerr AR, Silva NA, Mitchell TJ: Contribution of the ATP-dependent protease ClpCP to the autolysis and virulence of *Streptococcus pneumoniae*. *Infect Immun* 2005, 73:730–740
 41. Walker M, McArthur J, McKay F, Ranson M: Is plasminogen deployed as a *Streptococcus pyogenes* virulence factor? *Trends Microbiol* 2005, 13:308–313
 42. Levin JC, Wessels MR: Identification of *csrR/csrS*, a genetic locus that regulates hyaluronic acid capsule synthesis in group A *Streptococcus*. *Mol Microbiol* 1998, 30:209–219
 43. Heath A, DiRita VJ, Barg NL, Engleberg NC: A two-component regulatory system, *CsrR-CsrS*, represses expression of three *Streptococcus pyogenes* virulence factors, hyaluronic acid capsule, streptolysin S, and pyrogenic exotoxin B. *Infect Immun* 1999, 67:5298–5305
 44. Federle MJ, McIver KS, Scott JR: A response regulator that represses transcription of several virulence operons in the group A streptococcus. *J Bacteriol* 1999, 181:3649–3657
 45. Dalton TL, Scott JR: *CovS* inactivates *CovR* and is required for growth under conditions of general stress in *Streptococcus pyogenes*. *J Bacteriol* 2004, 186:3928–3937
 46. Overweg K, Kerr A, Sluiter M, Jackson MH, Mitchell TJ, de Jong APJM, de Groot R, Hermans PWM: The putative proteinase maturation protein A of *Streptococcus pneumoniae* is a conserved surface protein with potential to elicit protective immune responses. *Infect Immun* 2000, 68:4180–4188
 47. Hytonen J, Haataja S, Finne J: *Streptococcus pyogenes* glycoprotein-binding streptadhesin activity is mediated by a surface-associated carbohydrate-degrading enzyme, pullulanase. *Infect Immun* 2003, 71:784–793
 48. Shelburne III SA, Sumbly P, Sitkiewicz I, Granville C, DeLeo FR, Musser JM: Central role of a bacterial two-component gene regulatory system of previously unknown function in pathogen persistence in human saliva. *Proc Natl Acad Sci USA* 2005, 102:16037–16042
 49. Brunskill EW, Bayles KW: Identification and molecular characterization of a putative regulatory locus that affects autolysis in *Staphylococcus aureus*. *J Bacteriol* 1996, 178:611–618
 50. Titgemeyer F, Hillen W: Global control of sugar metabolism: a gram-positive solution. *Antonie Van Leeuwenhoek* 2002, 82:59–71
 51. Seki M, Iida K, Saito M, Nakayama H, Yoshida S: Hydrogen peroxide production in *Streptococcus pyogenes*: involvement of lactate oxidase and coupling with aerobic utilization of lactate. *J Bacteriol* 2004, 186:2046–2051
 52. Herwald H, Cramer H, Morgelin M, Russell W, Sollenberg U, Norrby-Teglund A, Flodgaard H, Lindbom L, Björck L: M protein, a classical bacterial virulence determinant, forms complexes with fibrinogen that induce vascular leakage. *Cell* 2004, 116:367–379
 53. Kapur V, Majesky M, Li L, Black R, Musser J: Cleavage of interleukin 1{beta} (IL-1{beta}) precursor to produce active IL-1{beta} by a conserved extracellular cysteine protease from *Streptococcus pyogenes*. *Proc Natl Acad Sci USA* 1993, 90:7676–7680
 54. Kapur V, Topouzis S, Majesky MW, Li LL, Hamrick MR, Hamill RJ, Patti JM, Musser JM: A conserved *Streptococcus pyogenes* extracellular cysteine protease cleaves human fibronectin and degrades vitronectin. *Microb Pathog* 1993, 15:327–346
 55. Svensson M, Scaramuzzino D, Sjöbring U, Olsen A, Frank C, Bessen D: Role for a secreted cysteine proteinase in the establishment of host tissue tropism by group A streptococci. *Mol Microbiol* 2000, 38:242–253
 56. Nyberg P, Rasmussen M, Björck L: {alpha}2-Macroglobulin-proteinase complexes protect *Streptococcus pyogenes* from killing by the antimicrobial peptide LL-37. *J Biol Chem* 2004, 279:52820–52823
 57. Fernie-King BA, Seilly DJ, Willers C, Wurznier R, Davies A, Lachmann PJ: Streptococcal inhibitor of complement (SIC) inhibits the membrane attack complex by preventing uptake of C567 onto cell membranes. *Immunology* 2001, 103:390–398
 58. Frick IM, Akesson P, Rasmussen M, Schmidtchen A, Björck L: SIC, a secreted protein of *Streptococcus pyogenes* that inactivates antibacterial peptides. *J Biol Chem* 2003, 278:16561–16566
 59. Brinkmann V, Reichard U, Goosmann C, Fauler B, Uhlemann Y, Weiss DS, Weinrauch Y, Zychlinsky A: Neutrophil extracellular traps kill bacteria. *Science* 2004, 303:1532–1535
 60. Miyoshi-Akiyama T, Takamatsu D, Koyanagi M, Zhao J, Imanishi K, Uchiyama T: Cytocidal effect of *Streptococcus pyogenes* on mouse neutrophils in vivo and the critical role of streptolysin S. *J Infect Dis* 2005, 192:107–116
 61. Li Z, Sledjeski DD, Kreikemeyer B, Podbielski A, Boyle MD: Identification of *pel*, a *Streptococcus pyogenes* locus that affects both surface and secreted proteins. *J Bacteriol* 1999, 181:6019–6027
 62. Mangold M, Siller M, Roppenser B, Vlamincx B, Penfound T, Klein R, Novak R, Novick R, Charpentier E: Synthesis of group A streptococcal virulence factors is controlled by a regulatory RNA molecule. *Mol Microbiol* 2004, 53:1515–1527
 63. Cockerill FR, Thompson R, Musser J, Schlievert P, Talbot J, Holley K, Harmsen W, Ilstrup D, Kohner P, Kim M, Frankfurt B, Manahan J, Steckelberg J, Roberson F, Wilson W: Molecular, serological, and clinical features of 16 consecutive cases of invasive streptococcal disease. Southeastern Minnesota Streptococcal Working Group. *Clin Infect Dis* 1998, 26:1448–1458
 64. Bhakdi S, Tranum-Jensen J, Sziegoleit A: Mechanism of membrane damage by streptolysin-O. *Infect Immun* 1985, 47:52–60
 65. Ruiz N, Wang B, Pentland A, Caparon M: Streptolysin O and adherence synergistically modulate proinflammatory responses of keratinocytes to group A streptococci. *Mol Microbiol* 1998, 27:337–346
 66. Limbago B, Penumalli V, Weinrick B, Scott JR: Role of streptolysin O in a mouse model of invasive group A streptococcal disease. *Infect Immun* 2000, 68:6384–6390
 67. Betschel SD, Borgia SM, Barg NL, Low DE, De Azavedo JCS: Reduced virulence of group A streptococcal Tn916 mutants that do not produce streptolysin S. *Infect Immun* 1998, 66:1671–1679
 68. Ginsburg I: Is streptolysin S of group A streptococci a virulence factor? *APMIS* 1999, 107:1051–1059
 69. Kobayashi SD, Braughton KR, Whitney AR, Voyich JM, Schwan TG, Musser JM, DeLeo FR: Bacterial pathogens modulate an apoptosis differentiation program in human neutrophils. *Proc Natl Acad Sci USA* 2003, 100:10948–10953
 70. Christ EA, Meals E, English BK: Streptococcal pyrogenic exotoxins A (SpeA) and C (SpeC) stimulate the production of inducible nitric oxide synthase (iNOS) protein in RAW 264.7 macrophages. *Shock* 1997, 8:450–453
 71. Cusumano V, Fera MT, Carbone M, Anzani Ciliberti F, Bellantoni A: Synergic activities of streptococcal pyrogenic exotoxin A and lipoteichoic acid in cytokine induction. *New Microbiologica* 2000, 23:37–45
 72. Rasmussen M, Müller HP, Björck L: Protein GRAB of *Streptococcus pyogenes* regulates proteolysis at the bacterial surface by binding alpha2-macroglobulin. *J Biol Chem* 1999, 274:15336–15344
 73. Lottenberg R, Desjardins L, Wang H, Boyle M: Streptokinase-producing streptococci grown in human plasma acquire unregulated cell-associated plasmin activity. *J Infect Dis* 1992, 166:436–440
 74. Sun H, Ringdahl U, Homeister JW, Fay WP, Engleberg NC, Yang AY, Rozek LS, Wang X, Sjöbring U, DG: Plasminogen is a critical host pathogenicity factor for group A streptococcal infection. *Science* 2004, 305:1283–1286
 75. Elsner A, Kreikemeyer B, Braun-Kiewnick A, Spellerberg B, Buttaro BA, Podbielski A: Involvement of Lsp, a member of the Lral lipoprotein family in *Streptococcus pyogenes*, in eukaryotic cell adhesion and internalization. *Infect Immun* 2002, 70:4859–4869
 76. Ji Y, McLandsborough L, Kondagunta A, Cleary PP: C5a peptidase alters clearance and trafficking of group A streptococci by infected mice. *Infect Immun* 1996, 64:503–510
 77. Hoe NP, Ireland RM, DeLeo FR, Gowen BB, Dorward DW, Voyich JM, Liu M, Burns EH, Culnan DM, Bretscher A, Musser JM: Insight into the molecular basis of pathogen abundance: group A *Streptococcus* inhibitor of complement inhibits bacterial adherence and internalization into human cells. *Proc Natl Acad Sci USA* 2002, 99:7646–7651
 78. Carlsson F, Berggard K, Stalhammar-Carlemalm M, Lindahl G: Evasion of phagocytosis through cooperation between two ligand-binding regions in *Streptococcus pyogenes* M protein. *J Exp Med* 2003, 198:1057–1068
 79. Frick IM, Schmidtchen A, Sjöbring U: Interactions between M proteins of *Streptococcus pyogenes* and glycosaminoglycans promote

- bacterial adhesion to host cells. *Eur J Biochem* 2003, 270:2303–2311
80. Carlsson F, Sandin C, Lindahl G: Human fibrinogen bound to *Streptococcus pyogenes* M protein inhibits complement deposition via the classical pathway. *Mol Microbiol* 2005, 56:28–39
81. Lukomski S, Sreevatsan S, Amberg C, Reichardt W, Woischnik M, Podbielski A, Musser JM: Inactivation of *Streptococcus pyogenes* extracellular cysteine protease significantly decreases mouse lethality of serotype M3 and M49 strains. *J Clin Invest* 1997, 99:2574–2580
82. Lukomski S, Burns EHJ, Wyde PR, Podbielski A, Rurangirwa J, Moore-Poveda DK, Musser JM: Genetic inactivation of an extracellular cysteine protease (SpeB) expressed by *Streptococcus pyogenes* decreases resistance to phagocytosis and dissemination to organs. *Infect Immun* 1998, 66:771–776
83. Cleary PP, Larkin A: Hyaluronic acid capsule: strategy for oxygen resistance in group A streptococci. *J Bacteriol* 1979, 140:1090–1097
84. Cywes C, Wessels M: Group A *Streptococcus* tissue invasion by CD44-mediated cell signalling. *Nature* 2001, 414:648–652
85. Kil KS, Cunningham MW, Barnett LA: Cloning and sequence analysis of a gene encoding a 67-kilodalton myosin-cross-reactive antigen of *Streptococcus pyogenes* reveals its similarity with class II major histocompatibility antigens. *Infect Immun* 1994, 62:2440–2449
86. Khil J, Im M, Heath A, Ringdahl U, Mundada L, Cary Engleberg N, Fay W: Plasminogen enhances virulence of group A streptococci by streptokinase-dependent and streptokinase-independent mechanisms. *J Infect Dis* 2003, 188:497–505
87. Yoshizawa N, Yamakami K, Fujino M, Oda T, Tamura K, Matsumoto K, Sugisaki T, Boyle MDP: Nephritis-associated plasmin receptor and acute poststreptococcal glomerulonephritis: characterization of the antigen and associated immune response. *J Am Soc Nephrol* 2004, 15:1785–1793
88. Oda T, Yamakami K, Omasu F, Suzuki S, Miura S, Sugisaki T, Yoshizawa N: Glomerular plasmin-like activity in relation to nephritis-associated plasmin receptor in acute poststreptococcal glomerulonephritis. *J Am Soc Nephrol* 2005, 16:247–254
89. Zimbelman J, Palmer A, Todd J: Improved outcome of clindamycin compared with beta-lactam antibiotic treatment for invasive *Streptococcus pyogenes* infection. *Pediatr Infect Dis J* 1999, 18:1096–1100
90. Gemmell C, Peterson P, Schmeling D, Kim Y, Mathews J, Wannamaker L, Quie P: Potentiation of opsonization and phagocytosis of *Streptococcus pyogenes* following growth in the presence of clindamycin. *J Clin Invest* 1981, 67:1249–1256
91. Sriskandan S, McKee A, Hall L, Cohen J: Comparative effects of clindamycin and ampicillin on superantigenic activity of *Streptococcus pyogenes*. *J Antimicrob Chemother* 1997, 40:275–277
92. Kotb M, Norrby-Teglund A, McGeer A, El-Sherbini H, Dorak M, Khurshid A, Green K, Peeples J, Wade J, Thomson G, Schwartz B, Low DE: An immunogenetic and molecular basis for differences in outcomes of invasive group A streptococcal infections. *Nat Med* 2002, 8:1398–1404
93. Kazmi SU, Kansal R, Aziz RK, Hooshdaran M, Norrby-Teglund A, Low DE, Halim AB, Kotb M: Reciprocal, temporal expression of SpeA and SpeB by invasive M1T1 group A streptococcal isolates in vivo. *Infect Immun* 2001, 69:4988–4995
94. Kansal RG, Aziz RK, Kotb M: Modulation of expression of superantigens by human transferrin and lactoferrin: a novel mechanism in host-*Streptococcus* interactions. *J Infect Dis* 2005, 191:2121–2129
95. Reid SD, Green NM, Sylva GL, Voyich JM, Stenseth ET, DeLeo FR, Palzkill T, Low DE, Hill HR, Musser JM: Postgenomic analysis of four novel antigens of group A *Streptococcus*: growth phase-dependent gene transcription and human serologic response. *J Bacteriol* 2002, 184:6316–6324
96. Degnan BA, Fontaine MC, Doebereiner AH, Lee JJ, Mastroeni P, Dougan G, Goodacre JA, Kehoe MA: Characterization of an isogenic mutant of *Streptococcus pyogenes* Manfredo lacking the ability to make streptococcal acid glycoprotein. *Infect Immun* 2000, 68:2441–2448
97. Degnan BA, Palmer JM, Robson T, Jones CED, Fischer M, Glanville M, Mellor GD, Diamond AG, Kehoe MA, Goodacre JA: Inhibition of human peripheral blood mononuclear cell proliferation by *Streptococcus pyogenes* cell extract is associated with arginine deiminase activity. *Infect Immun* 1998, 66:3050–3058
98. Gruening P, Fulde M, Valentin-Weigand P, Goethe R: Structure, regulation, and putative function of the arginine deiminase system of *Streptococcus suis*. *J Bacteriol* 2006, 188:361–369
99. Ravins M, Jaffe J, Hanski E, Shetzigovski I, Natanson-Yaron S, Moses AE: Characterization of a mouse-passaged, highly encapsulated variant of group A streptococcus in in vitro and in vivo studies. *J Infect Dis* 2000, 182:1702–1711
100. Raeder R, Harokopakis E, Hollingshead S, Boyle MD: Absence of SpeB production in virulent large capsular forms of group A streptococcal strain 64. *Infect Immun* 2000, 68:744–751
101. Engleberg CN, Heath A, Miller A, Rivera C, DiRita VJ: Spontaneous mutations in the CsrRS two-component regulatory system of *Streptococcus pyogenes* result in enhanced virulence in a murine model of skin and soft tissue infection. *J Infect Dis* 2001, 183:1043–1054
102. Gryllos I, Levin JC, Wessels MR: The CsrR/CsrS two-component system of group A *Streptococcus* responds to environmental Mg²⁺. *Proc Natl Acad Sci USA* 2003, 100:4227–4232
103. Voyich JM, Sturdevant DE, Braughton KR, Kobayashi SD, Lei B, Virtaneva K, Dorward DW, Musser JM, DeLeo FR: Genome-wide protective response used by group A *Streptococcus* to evade destruction by human polymorphonuclear leukocytes. *Proc Natl Acad Sci USA* 2003, 100:1996–2001
104. Caparon MG, Geist RT, Perez-Casal J, Scott JR: Environmental regulation of virulence in group A streptococci: transcription of the gene encoding M protein is stimulated by carbon dioxide. *J Bacteriol* 1992, 174:5693–5701
105. VanHeyningen T, Fogg G, Yates D, Hanski E, Caparon M: Adherence and fibronectin binding are environmentally regulated in the group A streptococci. *Mol Microbiol* 1993, 9:1213–1222
106. Smoot LM, Smoot JC, Graham MR, Somerville GA, Sturdevant DE, Migliaccio CA, Sylva GL, Musser JM: Global differential gene expression in response to growth temperature alteration in group A *Streptococcus*. *Proc Natl Acad Sci USA* 2001, 98:10416–10421
107. Kreikemeyer B, Boyle MD, Buttaro BA, Heinemann M, Podbielski A: Group A streptococcal growth phase-associated virulence factor regulation by a novel operon (Fas) with homologies to two-component-type regulators requires a small RNA molecule. *Mol Microbiol* 2001, 39:392–406
108. Kristian SA, Datta V, Weidenmaier C, Kansal R, Fedtke I, Peschel A, Gallo RL, Nizet V: D-Alanylation of teichoic acids promotes group A *Streptococcus* antimicrobial peptide resistance, neutrophil survival, and epithelial cell invasion. *J Bacteriol* 2005, 187:6719–6725
109. Deutscher J, Herro R, Bourand A, Mijakovic I, Poncet S: P-Ser-HPr—a link between carbon metabolism and the virulence of some pathogenic bacteria. *Biochim Biophys Acta* 2005, 1754:118–125
110. Boyce JD, Wilkie I, Harper M, Paustian ML, Kapur V, Adler B: Genomic scale analysis of *Pasteurella multocida* gene expression during growth within the natural chicken host. *Infect Immun* 2002, 70:6871–6879
111. Merrell DS, Butler SM, Qadri F, Dolganov NA, Alam A, Cohen MB, Calderwood SB, Schoolnik GK, Camilli A: Host-induced epidemic spread of the cholera bacterium. *Nature* 2002, 417:642–645
112. Xu Q, Dziejman M, Mekalanos JJ: Determination of the transcriptome of *Vibrio cholerae* during intrainestinal growth and midexponential phase in vitro. *Proc Natl Acad Sci USA* 2003, 100:1286–1291
113. Stintzi A, Marlow D, Palyada K, Naikare H, Panciera R, Whitworth L, Clarke C: Use of genome-wide expression profiling and mutagenesis to study the intestinal lifestyle of *Campylobacter jejuni*. *Infect Immun* 2005, 73:1797–1810
114. Conway T, Schoolnik GK: Microarray expression profiling: capturing a genome-wide portrait of the transcriptome. *Mol Microbiol* 2003, 47:879–889
115. Shelburne S, Musser J: Virulence gene expression in vivo. *Curr Opin Microbiol* 2004, 7:283–289
116. Boyce J, Cullen P, Adler B: Genomic-scale analysis of bacterial gene and protein expression in the host. *Emerg Infect Dis* 2004, 10:1357–1362